Effects of nucleosome stability on remodeler-catalyzed repositioning

Aaron M. Morgan, Sarah E. LeGresley, Koan Briggs, Gada Al-Ani, and Christopher J. Fischer

Phys. Rev. E **97**, 032422 — Published 30 March 2018

DOI: 10.1103/PhysRevE.97.032422

Effects of Nucleosome Stability on Remodeler-Catalyzed Repositioning

Aaron M. Morgan, Sarah E. LeGresley, Koan Briggs, Gada Al-Ani, and Christopher J. Fischer*
Department of Physics and Astronomy
University of Kansas
1251 Wescoe Hall Dr., 1082 Malott Hall
Lawrence, KS 66045 USA
785-864-4579
FAX: 785-864-5262
(Dated: March 6, 2018)

Chromatin remodelers are molecular motors that play essential roles in the regulation of nucleosome positioning and chromatin accessibility. These machines couple the energy obtained from the binding and hydrolysis of ATP to the mechanical work of manipulating chromatin structure through processes that are not completely understood. Here we present a quantitative analysis of nucleosome repositioning by the chromatin remodeler ISWI and demonstrate that nucleosome stability significantly impacts the observed activity. We show how DNA damage induced changes in the affinity of DNA wrapping within the nucleosome can affect ISWI repositioning activity and demonstrate how assay-dependent limitations can bias studies of nucleosome repositioning. Together, these results also suggest that some of the diversity seen in chromatin remodeler activity can be attributed to the variations in the thermodynamics of interactions between the remodeler, the histones, and the DNA, rather than reflect inherent properties of the remodeler itself.

* Corresponding author: shark@ku.edu

I. INTRODUCTION

The first step in the compaction of the eukaryotic genome into chromatin involves the wrapping (*i.e.*,bending) of the DNA around histone octamers to form nucleosomes [1–4]. Within each nucleosome, the wrapped DNA contacts the histone octamer at 14 different sites, spaced approximately 10 basepairs apart, each of which contains several different types of noncovalent interactions (van der Waals interactions, hydrogen bonds, *e.g.*) between the DNA and the histones [1, 3]. The histone octamer together with the ≈147 basepairs of nucleosomal DNA wrapped around it is referred to as the nucleosome core particle (NCP). Since the packaging of DNA into nucleosomes requires both that specific contacts be made between the DNA and the histones and that the DNA be wrapped/bent around the histone octamer [1–4], it is not surprising that the thermodynamic stability of a nucleosome depends upon the sequence of the nucleosomal DNA [5–9]. For example, sequences of DNA that can be more easily bent around the histone octamer display a higher affinity for octamer binding [10] and nucleosomes reconstituted using such DNA sequences are also more stable [10]. The periodicity of particular dinucleotides in DNA sequences with high affinity for binding the histone octamer further demonstrates the correlation between DNA sequence and nucleosome stability as the positions of these dinucleotides in the DNA increases the flexibility of the DNA, thereby lowering the energy barrier for wrapping the DNA around the histone octamer and also increasing the stability of the nucleosomes [5, 6, 10].

The packaging of DNA into nucleosomes restricts the ability of DNA binding proteins to access the wrapped nucleosomal DNA [11–13]. Consequently, DNA wrapping within nucleosomes must be dynamically controlled in order to regulate the accessibility of the packaged DNA to DNA repair, DNA replication, and gene expression machinery [14, 15]. One mechanism of control involves the activity of molecular motors called chromatin remodelers, which reposition NCPs along DNA (*i.e.*, move histone octamers relative to the DNA) using an ATP-dependent mechanism [16–18]. Several models have been proposed for this repositioning reaction, nearly all of which rely upon the ability of the chromatin remodeler to translocate along the nucleosomal DNA [16–24]. In order to shift the histone octamer relative to the DNA, this process of DNA transocation must be coupled with the breaking of existing histone:DNA contacts and the subsequent re-establishing of new histone:DNA contacts with the translocated DNA (a loop of DNA, *e.g.* [18, 21–25]). Since these processes also require the location and topology of the nucleosomal DNA to be altered, it is not surprising that the sequence of nucleosomal DNA has been shown to influence the nucleosome repositioning activity of chromatin remodelers [26–30].

Indeed, although nucleosomes are stable, they are nevertheless highly dynamic with the DNA being partially unwrapped from the histone octamer between 2% and 10% of the time [31]. Chromatin remodelers likely take advantage of these nucleosome dynamics for their repositioning activity [31] and may also influence them directly by competing with the histones for DNA binding [32, 33]; the binding of nucleosomal DNA by the histone octamer is also affected by remodeler binding induced distortions of the histone octamer [34]. This interplay between histone:DNA binding, remodeler:DNA binding, and remodeler:histone binding contributes to the observed rate of nucleosome repositioning and can account for the dependence of observed rates of repositioning on the sequence of the nucleosomal DNA [26–30]. Not only does this complicate our ability to discern the intrinsic repositioning activity of the remodeling motor itself (or even necessarily how one would define that activity), but more significantly, there is a risk that in some experiments the thermodynamics of histone:DNA interactions within the nucleosome can be rate-limiting for remodeler-catalyzed nucleosome requisitioning, especially for nucleosomes reconstituted with high-affinity nucleosome positioning sequences [5–7]. In other words, it is possible that experiments designed to analyze the repositioning activity of chromatin remodelers, may instead be reporting primarily on the affinity of histone:DNA interactions within the nucleosome rather than the activity of the remodeler itself. While this may be helpful in providing an alternative tool for measuring DNA:histone interactions (*i.e.*, an alternative probe of histone:DNA interaction free energy [6]), it clearly muddles what can be concluded about the intrinsic repositioning activity of the remodeler and how this activity is influenced by post-translational modifications, the presence of accessory proteins, *etc.*. To address this concern, we present here a mathematical model for remodeler-catalyzed nucleosome repositioning and demonstrate its application to both previously published and new data using the chromatin remodeler ISWI [35–38] as a categorical example. We show how this model can reconcile seemingly disparate characterizations of the ISWI's nucleosome repositioning activity, including estimates of the number of processes associated with this reaction (and corresponding rate constants) as well as the influence of substrate and assay design on measurements of this activity. Finally, we offer a quantitative discussion on the influence of DNA damage on nucleosome repositioning. Taken together, these results suggest a systematic strategy for future studies seeking to characterize the intrinsic activity of chromatin remodelers.

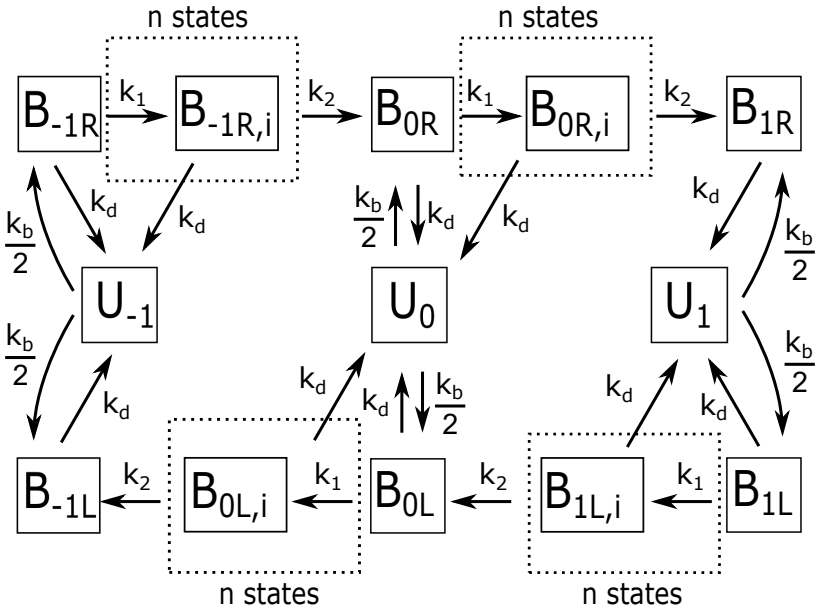

FIG. 1: Nucleosome repositioning model with three octamer binding sites on the DNA. Transitions between binding sites occur through n sequential repeats of a process with rate constant k_1 followed by a single process with rate constant k_2. The variables k_d and k_b denote the microscopic dissociation and binding constants, respectively, for a remodeler interacting with the nucleosome.

II. MATHEMATICAL MODEL FOR NUCLEOSOME REPOSITIONING

It has been suggested that the very poor efficiency with which the ISWI chromatin remodeler couples ATP hydrolysis to nucleosome repositioning results from ISWI engaging in multiple rounds of 'futile repositioning' for each successful repositioning event [27]; this explanation is also consistent with observations that ISWI repositions nucleosomes through a random-walk mechanism [27]. In this mechanism, the probability of successful repositioning is so low that the location of a histone octamer is shifted, on average, only to the nearest translational position along the DNA before ISWI dissociates from it. When the octamer is next bound by ISWI, there will be no 'memory' of the previous direction of repositioning and thus an equal probability that ISWI will attempt to move the octamer in either direction along the DNA [27].

To explore the implications of multiple rounds of futile repositioning further, we propose that each successful repositioning reaction consists of two different ATP-dependent processes; similar models have been previously proposed in one form or another [21–24]. Specifically, we propose that successful repositioning consists of (several possible rounds of) remodeler translocation along the nucleosomal DNA followed by a single event in which the remodeler *resets* the nucleosome by (i) breaking existing histone:DNA contacts, (ii) bending and shifting the translocated DNA (possibly in the form of a wave or bulge [18, 21–24, 33]) to its new location relative to the histone octamer, and (iii) possibly assisting in the establishment of new histone contacts with the shifted DNA. Failure by the remodeler to complete this final event before ISWI dissociation results in the translocated DNA resettling to its previous position with respect to the histone octamer and re-establishing the associated histone:DNA contacts. According to this model, if either the processivity of DNA translocation is low (such that the remodeler cannot complete all required DNA translocation before dissociating from the nucleosome) or if the probability of completing the final process of repositioning is low (such that the remodeler cannot complete it before dissociating from the nucleosome), multiple 'futile' rounds of ATP-coupled DNA translocation will be associated with each successful repositioning event. This would naturally inflate the amount of ATP associated with repositioning and thus make nucleosome repositioning appear less energy efficient (in terms of ATP hydrolysis) than it actually is.

We begin by considering a model in which the histone octamer can be located in three positions on the DNA [27]; these positions correspond to minimum energy states for the interactions of the histone octamer with the DNA. Transitions between these states occur through a combination of n sequential DNA translocation processes, each associated with a microscopic rate constant k_1 followed by a single process, associated with the microscopic rate constant k_2, that accounts for all non-translocation processes related to nucleosome repositioning (bending or otherwise changing the topology of the DNA, breaking and re-establishing of histone:DNA contacts, *e.g.*). In this

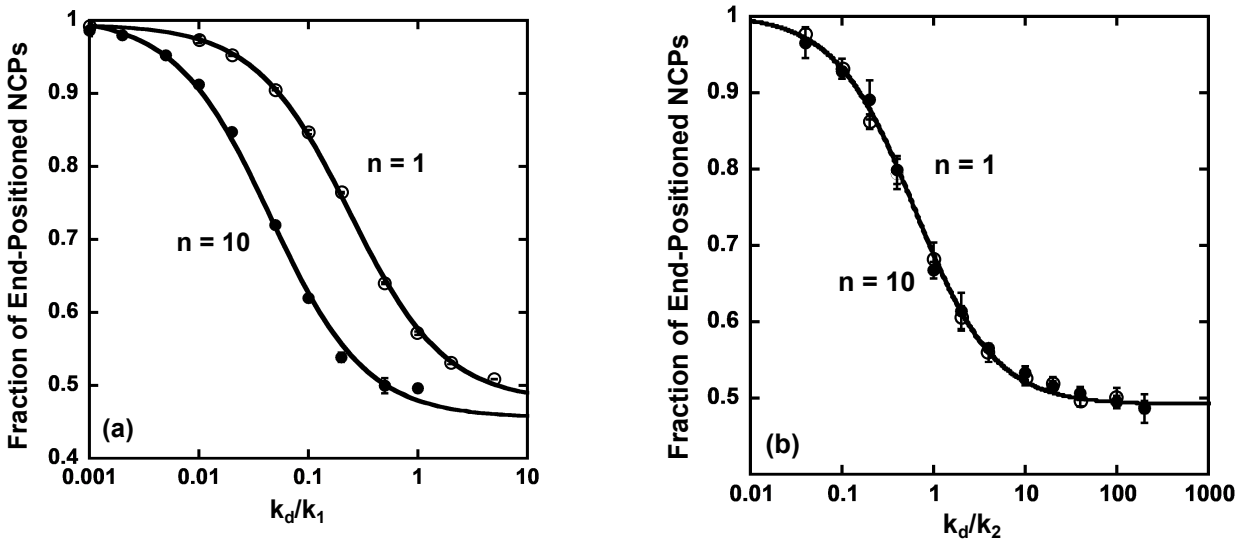

FIG. 2: Fraction of end-positioned NCPs as a function of k_d/k_1 (a) or k_d/k_2 (b) from simulations using the model in Fig. 1 for $n = 1$ (open circles) and $n = 10$ (solid circles). The solid lines in the figure are theoretical curves determined from the differential equations describing the model in Fig. 1 using the same values for the parameters in that model as used in the simulations. Simulations when $k_2 \gg k_d$ (a) result in k_1 becoming rate limiting for the reaction when $k_d \gg k_1$, while simulations when $k_1 \gg k_d$ (b) result in k_2 becoming rate limiting for the reaction when $k_d \gg k_2$.

model, shown in Fig. 1, we assume that the repositioning reaction can proceed in either direction along the DNA, denoted as left (L) and right (R) in Fig. 1, depending upon the initial binding configuration of the remodeler with respect to the nucleosome. The subscripts -1, 0, and 1 in Fig. 1 denote the binding position of the octamer on the DNA; position 0 is the center position on the DNA. The populations U_{-1}, U_0, U_1 denote nucleosomes with octamers at binding positions -1, 0, and 1, respectively, which are not bound by remodelers. The populations B_x denote a nucleosome bound by a remodeler with the subscript x denoting the position of the octamer on the DNA and the direction of repositioning by the remodeler. Thus, the population B_{-1R} denotes nucleosomes bound by remodelers that are actively moving the histone octamers from position -1 toward the right (*i.e.*, toward position 0). The variables k_d and k_b denote the microscopic dissociation and binding constants, respectively, for a remodeler interacting with a nucleosome. As shown in Fig. 1, all transitional repositioning states ($B_{-1R,i}$, $B_{0R,i}$, $B_{0L,i}$, and $B_{1L,i}$) will dissociate to the previous configuration (*i.e.*, octamer binding position) if the process associated with rate constant k_2 is not completed before remodeler dissociation.

We show in Fig. 2 the results of Monte Carlo simulations of time courses of nucleosome repositioning using the model shown in Fig. 1 (see Materials and Methods). In Fig. 2, we plot the fraction of end-positioned NCPs (*i.e.*, the fraction which are B_{-1L}, B_{-1R}, U_{-1}, B_{1R}, B_{1L}, U_1, $B_{1L,i}$, and $B_{-1R,i}$) for systems in which the process associated with k_1 is varied [Fig. 2(a)] or the process associated with k_2 is varied [Fig. 2(b)] for two different values of n. For all simulations, as the magnitude of $\frac{k_d}{k_1}$ or $\frac{k_d}{k_2}$ increases, the associated processes (k_1 or k_2) become rate-limiting for the repositioning reaction. As a result, as the magnitude $\frac{k_d}{k_1}$ [Fig. 2(a)] or $\frac{k_d}{k_2}$ [Fig. 2(b)] increases, the fraction of end-positioned NCPs approaches one-half, as expected for a random walk [39]. In contrast, as the magnitude of k_1 or k_2 increases, the fraction of end-positioned NCPs approach one. In this case, the NCPs are continually repositioned the entire length of the DNA following each binding of the remodeler. As expected, in cases where k_1 is rate-limiting [Fig. 2(a)], *i.e.*, when DNA translocation is rate-limiting for the repositioning reaction, the midpoint of the transition depends upon the number of intermediate steps n in the repositioning reaction. As shown in Fig. 2(a), the midpoint shifts to a smaller value of k_d/k_1 as n increases. Whereas in cases where k_2 is rate-limiting, there is no dependence of the transition on n [Fig. 2(b)].

We solved the differential equations associated with the model shown in Fig. 1 assuming that the microscopic binding constant k_b can be determined from the concentration of free remodeler in the reaction, denoted by $[R]$ and the equilibrium dissociation constant of the nucleosome:remodeler interaction, denoted as K_D, as shown in Eq. 1.

$$k_b = \Big(\frac{[R]}{K_D}\Big)k_d \tag{1}$$

When either k_1 or k_2 is rate-limiting, the time courses of repositioning derived from the model in Fig. 1 can be modeled as a random walk. As shown in the Appendix, when k_1 is rate-limiting the effective rate constant for this random walk, $k_{eff,1}$ is defined by Eq. 2.

$$k_{eff,1} \equiv k_d\Big(\frac{[R]}{[R]+K_D}\Big)\Big(\frac{k_1}{k_1+k_d}\Big)^n \tag{2}$$

When k_2 is rate limiting, the effective rate constant, $k_{eff,2}$, is defined by Eq. 3.

$$k_{eff,2} \equiv k_2\Big(\frac{[R]}{[R]+K_D}\Big)\Big(\frac{k_1}{k_1+k_d}\Big)^n \tag{3}$$

For the system consisting of three total binding sites for the histone octamer shown in Fig. 1, if we assume that all NCPs are initially located at the center of the DNA (*i.e.*, at position 0 in Fig. 1), and that the repositioning reaction proceeds through a random walk, then the population of NCPs at either of the ends of the DNA (*i.e.*, at position -1 or position 1 in Fig. 1) is described by Eq. 4 and the population of NCPs at position 0 is described by Eq. 5. The variable k_{eff} in these equations can be either $k_{eff,1}$ (Eq. 2) or $k_{eff,2}$ (Eq. 3) depending upon which process is rate-limiting for the reaction.

$$\frac{1}{4}\left(1 - e^{-2k_{eff}t}\right) \tag{4}$$

$$\frac{1}{2}\left(1 + e^{-2k_{eff}t}\right) \tag{5}$$

The model shown in Fig. 1 can be readily extended into the model shown in Fig. 3 in which there are two histone octamer binding positions on either side of the center binding position on the DNA. If we assume that repositioning proceeds through a random walk with all NCPs initially at position 0 (at time $t = 0$), then the population of NCPs at either of the ends of the DNA (*i.e.*, at position -2 or position 2 in Fig. 3) is described by Eq. 6.

$$\frac{1}{8}\left(e^{-2k_{eff}t}(e^{k_{eff}t} - 1)^2\right) \tag{6}$$

Similarly, under these conditions the population at position 0 is described by Eq. 7 and the population at either of the intermediate states (at position 1 or position -1 in Fig. 3) is described by Eq. 8.

$$\frac{1}{4}\left(e^{-2k_{eff}t}\Big(e^{k_{eff}t} + 1\Big)^2\right) \tag{7}$$

$$\frac{1}{4}\left(1 - e^{-2k_{eff}t}\right) \tag{8}$$

As before, the variable k_{eff} in Eq. 6 through Eq. 8 can be either $k_{eff,1}$ (Eq. 2) or $k_{eff,2}$ (Eq. 3) depending upon which process is rate-limiting for the reaction. It follows from Eq. 3 through Eq. 8 that the probability the remodeler will successfully shift the histone octamer by 1 binding position along the DNA before dissociating from the nucleosome is given by the following equation:

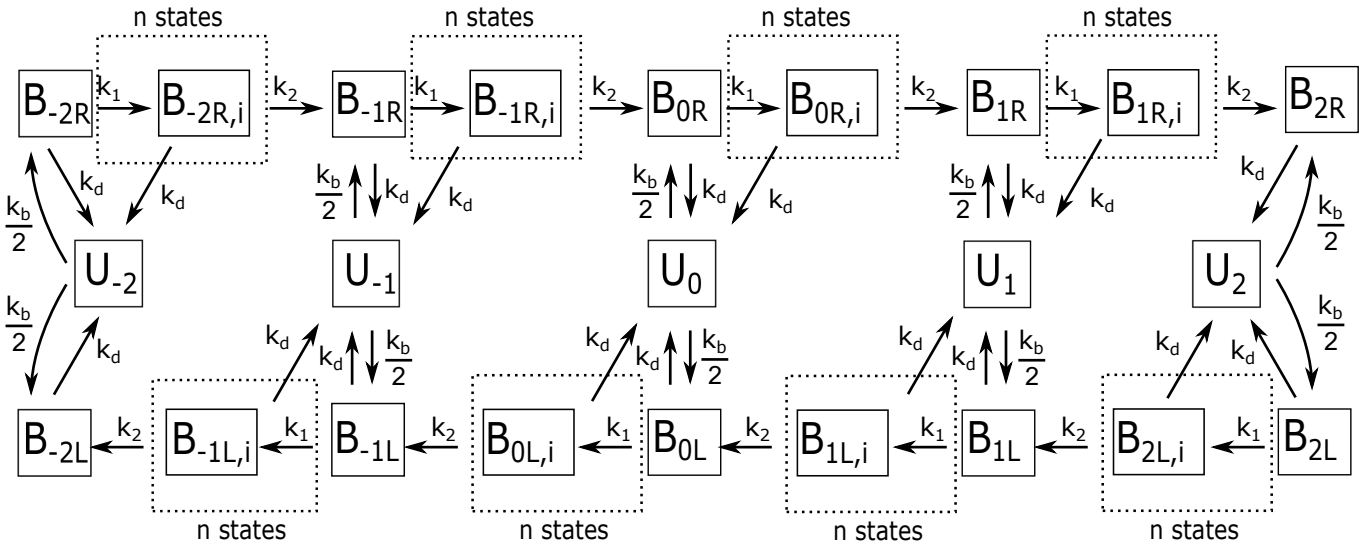

FIG. 3: Nucleosome repositioning model with five octamer binding sites on the DNA. Transitions between binding sites occur through n sequential repeats of a process with rate constant k_1 followed by a single process with rate constant k_2. The variables k_d and k_b denote the microscopic dissociation and binding constants, respectively, for a remodeler interacting with the nucleosome

$$\left(\frac{k_2}{k_2+k_d}\right)\left(\frac{k_1}{k_1+k_d}\right)^n \tag{9}$$

Therefore, the average number of futile repositioning events associated with each successful repositioning event, denoted as N_{fut}, is given by Eq. 10.

$$N_{fut} = \left(\frac{k_2+k_d}{k_2}\right)\left(\frac{k_1+k_d}{k_1}\right)^n - 1 \tag{10}$$

As discussed previously [27], the rate of ATP hydrolysis by the remodeler is independent of the number of histone binding sites on the DNA, but does, of course, depend upon the concentration of remodeler bound to nucleosomes. As shown in the Appendix, for the systems shown in Fig. 1 and Fig. 3, the rate of ATP hydrolysis (*i.e.*, ADP production) per nucleosome-bound remodeler is described by Eq. 11.

$$[ADP](t) = \left(k_1 + \frac{k_d(k_2-k_1)\left(\frac{k_1}{k_1+k_d}\right)^n}{k_d + k_2\left(1-\left(\frac{k_1}{k_1+k_d}\right)^n\right)}\right)t \tag{11}$$

In this derivation we have assumed that a single ATP molecule is hydrolyzed (a single ADP molecule produced) with each occurrence of the processes associated with the rate constants k_1 and k_2. To test the validity of these expressions, we performed Monte Carlo Simulations to generate time courses of nucleosome repositioning (octamer position and associated ATPase activity) and subsequently analyzed these data using Eq. 4, Eq. 6, and Eq. 11. As expected from the results shown in Fig. 2(a) and Fig. 2(b), these time courses were well described using Eq. 3 when $k_2 \gg k_d$ and $k_1 \lesssim k_d$ and Eq. 2 when $k_d \gg k_2$ and $k_1 \gg k_d$.

Lastly, it is worth noting that the derivation of Eq. 1 through Eq. 11 is predicated on the assumption that the affinity of NCP binding by the chromatin remodeler is independent of the concentration of nucleotide (ATP and/or ADP) in solution, as has been observed for ISWI [38]. If the affinity of NCP binding is dependent upon the nucleotide binding, we can replace the dissociation rate constant k_d in these equations with the expression shown in Eq. 12.

$$k_d = \frac{k_{d,0}K_A + [A]k_{d,\infty}}{[A]+K_A} \tag{12}$$

The variables $k_{d,0}$ and $k_{d,\infty}$ in Eq. 12 denote the dissociation rate constants in the absence of nucleotide and in the presence of saturating concentrations of nucleotide, respectively. The variable K_A is the equilibrium dissociation constant for nucleotide binding and the variable $[A]$ is the concentration of free nucleotide in solution.

III. DNA SEQUENCE EFFECTS

In our previously published study of ISWI-catalyzed nucleosome repositioning, we reported an apparent repositioning rate constant of $0.0247 min^{-1}$ and associated ATPase rate of $22 \frac{ATP}{min}$ per NCP-bound remodeler [27]. We speculated that the poor efficiency displayed by ISWI for coupling ATPase activity to repositioning (890 ATPs consumed per successful repositioning event [27]) indicated that multiple rounds of futile repositioning (and associated futile ATP hydrolysis) are associated with each successful repositioning event. To explore this further, we have reanalyzed these previously published results [27] using the models shown in Fig. 1 and Fig. 3 to determine estimates of the associated kinetic parameters. We note that a range of possible values for k_d for these models can be determined from the equilbirium dissociation constant $K_D = 1.3nM$ we determined for nucleosome binding by ISWI [38]. Assuming an association rate of $10^6 M^{-1}s^{-1}$ to $10^8 M^{-1}s^{-1}$ [40], we estimate that k_d can vary between $0.078 min^{-1}$ and $7.8 min^{-1}$.

We first consider the possibility that k_1 (*i.e.*, DNA translocation) is rate-limiting for the repositioning reaction. We further assume that a single ATP molecule is consumed for each process associated with rate constant k_1 and a single ATP molecule is consumed for each process associated with rate constant k_2. Substitution of our results into Eq. 3 and Eq. 11 gives us the following two expressions:

$$k_d\Big(\frac{k_1}{k_1+k_d}\Big)^n = (0.0247 \pm 0.0018) min^{-1} \tag{13}$$

$$\left(k_1 + \frac{k_d(k_2-k_1)\big(\frac{k_1}{k_1+k_d}\big)^n}{k_d + k_2\Big(1-\big(\frac{k_1}{k_1+k_d}\big)^n\Big)}\right) = (22 \pm 2)\frac{ATP}{min} \tag{14}$$

We can estimate values for n and k_1 from our previously determined DNA translocation rate of $300 \frac{basepairs}{min}$ for ISWI [41]. If we assume that 10 basepairs of nucleosomal DNA must be translocated by ISWI for each occurrence of the slow process associated with rate constant k_2 [27], then the value of k_1 will vary with n. For example, if $n = 10$, k_1 corresponds to the translocation of a single basepair of DNA and would therefore be equal to 300 min^{-1}. Similarly, if $n = 1$, k_1 corresponds to the translocation of 10 basepairs of DNA and is equal to $30 min^{-1}$. Using this constraint for k_1 we simultaneously solved Eq. 13 and Eq. 14 to determine estimates of k_d and k_2 for each value of n. For every value of n, there were no solutions where both k_d and k_2 were real and positive. It is reasonable to assume, of course, that ISWI's rate of DNA translocation is lower when the DNA is wrapped within an NCP than when the DNA is free in solution. We therefore determined estimates for k_2 and k_d for different values of n and decreasing values of k_1. Again, we discovered that there are no real and positive solutions for k_2 and k_d for any values of n and k_1. Therefore, we conclude that a model in which DNA translocation (k_1) is energetically rate-limiting for nucleosome repositioning by ISWI does not agree with empirical results.

We next determined values of k_2 and k_d assuming that k_2 was rate-limiting for the repositioning reaction. As before, we assume that a single ATP molecule is consumed for each process associated with rate constant k_1 and a single ATP molecule is consumed for each process associated with rate constant k_2. Equation 14 is still valid when k_2 is rate-limiting and we determine the second equation for our analysis by substituting our results into Eq. 2.

$$k_2\Big(\frac{k_1}{k_1+k_d}\Big)^n = (0.0247 \pm 0.0018) min^{-1} \tag{15}$$

As before, we determined values of k_2 and k_d using estimates of n and k_1 from our previously published DNA translocation studies [41]. These results, shown in Table I, indicate that only values of $n \geq 4$ are consistent with the affinity of the ISWI:nucleosome interaction [38]. As mentioned before, it is reasonable to assume that the rate of DNA translocation by ISWI will likely be slower when the DNA is wrapped around the histone octamer (or otherwise interacts with the histone octamer) than when it is free in solution, as was the case in our previously studies [41]. Therefore, the minimum value of n might be even larger than the results in Table I indicate. Furthermore, based upon the correlation between the parameters in Eq. 14 and Eq. 15 we know that the estimates of k_d and k_2 in Table I represent minimum and maximum values, respectively.

TABLE I: Estimates of k_d and k_2 for ISWI-catalyzed nucleosome repositioning [27] using the models shown in Fig. 1 and Fig. 3 (Eq. 14 and Eq. 15). The parameter n denotes the number of k_1 processes associated with each occurrence of a k_2 process in these models. For these calculations the value of k_1 was fixed using ISWI's rate of DNA translocation [41] and assuming that 10 basepairs of DNA must be translocated for the total n DNA translocation steps. The parameter N_{fut} is determined using Eq. 10 and the parameter N_{trans} is determined using Eq. 22.

n	$k_1(min^{-1})$	$k_d(min^{-1})$	$k_2(min^{-1})$	N_{fut}	N_{trans}
1	30	90 ± 30	0.10 ± 0.02	4000 ± 2000	1.38 ± 0.14
2	60	15.4 ± 1.8	0.039 ± 0.003	620 ± 110	4.9 ± 0.5
3	90	8.8 ± 0.9	0.033 ± 0.002	350 ± 50	11.2 ± 1.0
4	120	6.2 ± 0.6	0.030 ± 0.002	250 ± 30	20.4 ± 1.9
5	150	4.8 ± 0.4	0.029 ± 0.002	194 ± 23	32 ± 3
6	180	3.9 ± 0.4	0.028 ± 0.002	160 ± 20	47 ± 5
7	210	3.3 ± 0.3	0.028 ± 0.002	132 ± 16	65 ± 6
8	240	2.9 ± 0.3	0.027 ± 0.002	118 ± 16	84 ± 9
9	270	2.5 ± 0.2	0.027 ± 0.002	101 ± 11	109 ± 9
10	300	2.3 ± 0.2	0.027 ± 0.002	92 ± 11	131 ± 11

TABLE II: Estimates of $k_{d,critical}$ for ISWI-catalyzed nucleosome repositioning [27] using the models shown in Fig. 1 and Fig. 3 (Eq. 14 and Eq. 15). The parameter n denotes the number of k_1 processes associated with each occurrence of a k_2 process in these models. The parameter N_{fut} is determined using Eq. 10.

n	$k_{d,critical}$	$N_{fut,minimum}$
1	22 ± 2	900 ± 100
2	11 ± 1	450 ± 50
3	7.3 ± 0.7	300 ± 40
4	5.5 ± 0.5	220 ± 30
5	4.4 ± 0.4	180 ± 20
6	3.7 ± 0.3	150 ± 20
7	3.1 ± 0.3	130 ± 20
8	2.7 ± 0.2	110 ± 10
9	2.4 ± 0.2	100 ± 10
10	2.2 ± 0.2	90 ± 10

When k_2 is rate-limiting, simultaneous solutions of Eq. 14 and Eq. 15 give positive solutions for k_1 only when $k_d > k_{d,critical}$; positive solutions for k_2 exist for values of k_d above or below $k_{d,critical}$. The value of $k_{d,critical}$ depends upon n as shown in Table II. ISWI-catalyzed repositioning should be maximally efficient (*i.e.*, lowest value of N_{fut}) when $k_d = k_{d,critical}$ since that corresponds to $k_1 = \infty$ and $k_2 = 0.0247\ min^{-1}$. However, as shown in Table II, even under these conditions of maximal efficiency, less than approximately 1% of repositioning reactions are successful. Furthermore, the results in Table II indicate that $k_{d,critical}$ is less than the maximum value of k_d determined from the affinity of the ISWI:nucleosome interaction [38] for $n \geq 3$.

To examine the worse case scenario (least efficient repositioning), we determined values of k_1 and k_2 for Eq. 14 and Eq. 15 assuming the maximum value of $k_d = 7.8\ min^{-1}$; a maximum value of k_d will correspond to a minimum value of k_1, a maximum value of k_2, and a maximum value for N_{fut}. These results, shown in Table III, are also consistent with a value of $n \geq 4$ for ISWI-catalyzed nucleosome repositioning; no real and positive values for k_1 and k_2 are possible when $n < 3$ and the rate of DNA translocation when $n = 3$ exceeds what is observed for free DNA [41]. Finally, since the maximum values of k_1 in Table III are lower than what would be anticipated based upon ISWI's rate of DNA translocation (Table I) [41], these results suggest that ISWI's ability to translocation along DNA is impaired when the DNA is wrapped within an NCP. Lastly, these results indicate that less than 1% of repositioning reactions are successful.

The results in Table I and Table III are consistent with the hypothesis that multiple rounds of futile repositioning are associated with each successful repositioning event and that a process other than DNA translocation is energetically rate-limiting for the repositioning reaction. Indeed, the best case scenario for these calculations (*i.e.*, most efficient repositioning) indicate that approximately only 1% of repositioning reactions are successful, whereas some collections of parameters indicate that only 0.1% of repositioning reactions are successful. Such a low success rate for repositioning seems woefully inadequate for a machine tasked with respositioning nucleosomes and supports our hypothesis that the high affinity of histone binding by the nucleosomal DNA is unduly hindering ISWI's ability to reposition the nucleosomes [27]. Thus, the estimated values of k_2 reported in Table I might be more strongly influ-

TABLE III: Estimates of minimum value of k_1 and the maximum value k_2 for ISWI-catalyzed nucleosome repositioning [27] using the models shown in Fig. 1 and Fig. 3 (Eq. 14 and Eq. 15) assuming the maximum value of $k_d = 7.8min^{-1}$. The parameter n denotes the number of k_1 processes associated with each occurrence of a k_2 process in these models. The parameter N_{fut} is determined using Eq. 10 and the parameter N_{trans} is determined using Eq. 22. These parameters correspond to the least efficient repositioning possible (*i.e.*, maximum value of N_{fut}) for Eq. 14, Eq. 15, and $K_D = 1.3nM$ [38].

n	$k_{1,min}(min^{-1})$	$k_{2,max}(min^{-1})$	$N_{fut,maximum}$	N_{trans}
3	230 ± 90	0.027 ± 0.003	320 ± 40	32 ± 10
4	49 ± 12	0.044 ± 0.007	320 ± 70	7.3 ± 1.8
5	34 ± 6	0.069 ± 0.012	320 ± 80	5.4 ± 0.8
6	29 ± 4	0.10 ± 0.02	330 ± 90	4.7 ± 0.5
7	26 ± 3	0.15 ± 0.03	330 ± 90	4.3 ± 0.4
8	24 ± 3	0.22 ± 0.06	350 ± 120	4.1 ± 0.4
9	24 ± 2	0.33 ± 0.11	310 ± 110	4.1 ± 0.3
10	23 ± 2	0.38 ± 0.17	400 ± 190	4.0 ± 0.3

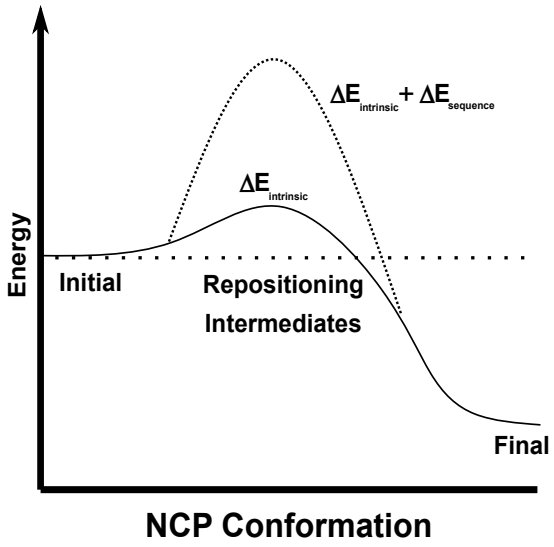

FIG. 4: The energy barrier to repositioning is a sum of contributions from the intrinsic energy barrier ($\Delta E_{intrinsic}$) associated with the biophysics of the remodeler interaction with the nucleosome and a DNA sequence specific energy barrier ($\Delta E_{sequence}$) related to DNA sequence changes to NCP stability.

enced by the thermodynamics of the histone:DNA interactions (bending or otherwise changing the topology of the DNA, breaking and re-establishing of histone:DNA contacts, *e.g.*) than by the intrinsic nucleosome repositioning activity of ISWI. Determining this latter activity would require determining values of k_2 for ISWI repositioning nucleosomes reconstituted with different DNA sequences with different affinities for wrapping the histone octamer and then analyzing the dependence of k_2 on nucleosome stability (free energy of DNA wrapping within the NCP [5, 6], *e.g.*). As shown in Fig. 4, we anticipate that the intrinsic energy barrier associated with nucleosome repositioning, corresponding to the ability of the remodeler to bind the nucleosome, distort the histone octamer, break and reform electrostatic interactions between the histones and the DNA, *etc.* can be increased by strengthening the affinity of the nucleosomal DNA for wrapping within the NCP.

We will assume that only k_2 is significantly affected by changes in DNA sequence and that the values of k_2 for different DNA sequences can be related using the simple Boltzmann statistics in Eq. 16.

$$\frac{k_{2,A}}{k_{2,B}} = e^{\Delta E_B - \Delta E_A} \tag{16}$$

The variable ΔE_A in Eq. 16 is the energy barrier associated with repositioning nucleosomes reconstituted with DNA sequence A and ΔE_B in Eq. 16 is the energy barrier associated with repositioning nucleosomes reconstituted with

DNA sequence B. As shown in Fig. 4, these energy barriers are the sum of an intrinsic energy barrier ($\Delta E_{intrinsic}$), associated with the biophysics of the remodeler interaction with the nucleosome, and a DNA sequence specific energy barrier ($\Delta E_{sequence}$), related to DNA sequence changes to NCP stability. Since $\Delta E_{intrinsic}$ should be unaffected by a change in DNA sequence we have

$$\Delta E_B - \Delta E_A = (\Delta E_{intrinsic,B} + \Delta E_{sequence,B}) - (\Delta E_{intrinsic,A} + \Delta E_{sequence,A})$$

$$\Delta E_B - \Delta E_A = \Delta E_{sequence,B} - \Delta E_{sequence,A} = \Delta\Delta E_{sequence}$$

$$\frac{k_{2,A}}{k_{2,B}} = e^{\Delta\Delta E_{sequence}} \tag{17}$$

We next sought to examine the validity of Eq. 17 empirically by monitoring the repositioning of nucleosomes reconstituted with different sequences of DNA. When analyzed using native gel electrophoresis, the electrophoretic mobility of a nucleosome is affected by the length DNA flanking the histone octamer, with octamers flanked symmetrically by equal lengths of DNA displaying the slowest gel mobility [27, 42]. Thus, a repositioning of the histone octamer relative to the DNA will result in a change in the electrophoretic mobility of the associated nucleosome. We used the chromatin remodeler ISWI for these experiments due to our past experience with this enzyme [27, 38, 41].

In order to break the assumption $k_d \gg k_2$ of the random walk model (Fig. 2), the values of k_2 in Table I and Table III would need to increase by around two orders of magnitude. According to Eq. 17, that change in k_2 would correspond to $\Delta\Delta E_{sequence} = 4.6 k_B T$. As a preliminary test of this hypothesis, we monitored the ISWI-catalyzed repositioning of nucleosomes reconstituted using 289 basepairs of random sequence DNA (see Materials and Methods); the difference in affinity of wrapping the histone octamer between the Widom 601 sequence (used in experiments associated with the parameters in Table I and Table III [27]) and random DNA is $(4.4 \pm 0.3) k_B T$ [6]. As shown in Fig. 5, four bands appear in the electrophoretic mobility shift assay of the corresponding repositioning reaction; we number these bands 1 through 4 from top to bottom in the lane. The relative intensities of the middle two bands (band 2 and band 3) are constant throughout the repositioning reaction whereas the relative intensities of band 1 and band 4 change with time. As indicated in Fig. 5, band 1 has roughly the same mobility as the center-positioned nucleosome reconstituted with the Widom 601 sequence. Similarly, band 4 has roughly the same mobility as the nucleosome with the most asymmetric lengths of flanking DNA occurring when ISWI repositions nucleosomes reconstituted with the Widom 601 sequence. We therefore ascribe band 1 and band 4 to center-positioned and end-positioned NCPs, respectively. As shown in Fig. 6, the intensity of band 1 decreases and the intensity of band 4 increases with time in the presence of ISWI and ATP. These time courses of band intensity are both well described by a single exponential change with associated rate constants of $(0.054 \pm 0.015) min^{-1}$ for band 1 and $(0.074 \pm 0.010) min^{-1}$ for band 4. The similarity of these rate constants and the anti-correlated changes in band intensity are consistent with ISWI repositioning the population of NCPs at the position associated with band 1 to the position associated with band 4.

Since the time courses in Fig. 6 are well described by a single exponential, the transition between center-positioned NCPs (band 1) and end-positioned NCPs (band 4) appears to proceed through a single step process. This is different from the six position random walk observed for ISWI-catalyzed repositioning of nucleosomes reconstituted with a similar length of DNA containing the Widom 601 sequence [27]. Similarly, while center-positioned NCPs remained the dominant observed species for a random walk [27, 39], the population of center-positioned NCPs in the reactions shown in Fig. 5 decrease to the smallest fraction of all observed species at the end of the reaction.

We show in Fig. 7 simulated time courses of the ISWI-catalyzed repositioning of nucleosomes reconstituted with different DNA sequences (in each case the DNA was 289 basepairs in length). The repositioning of nucleosomes reconstituted with random sequence DNA occurs 30 times faster than the repositioning of nucleosomes reconstituted with the Widom 601 sequence; for the latter simulations we assumed that repositioning occurred through a six position random walk using the previously determined apparent rate constant for ISWI-catalyzed nucleosome repositioning [27]. It is possible, however, that lowering the energy barrier to repositioning through a change of DNA sequence also allows ISWI to reposition the nucleosome through a sequential n-step mechanism [43], rather than through a random walk. Indeed, coarse grain molecular modeling of nucleosome repositioning indicates that the mechanism of repositioning is strongly linked to the sequence of the nucleosomal DNA due to the influence of DNA sequence on the free-energy of DNA wrapping within the NCP [30]. The corresponding six step sequential repositioning time course using the previously determined apparent rate constant for repositioning [27], still proceeds a factor of 20 more slowly than what is empirically observed in Fig. 5 and Fig. 6. This suggests that changing the sequence of the nucleosomal DNA has also changed the mechanism (rates, intermediates, *etc.*) of ISWI-catalyzed nucleosome repositioning, as expected from computer simulations [30]. Furthermore, since the apparent rate of repositioning changed by less than the factor of $\approx (80 \pm 20)$ estimated from the change of $(4.4 \pm 0.3) k_B T$ in DNA wrapping affinity, the observed

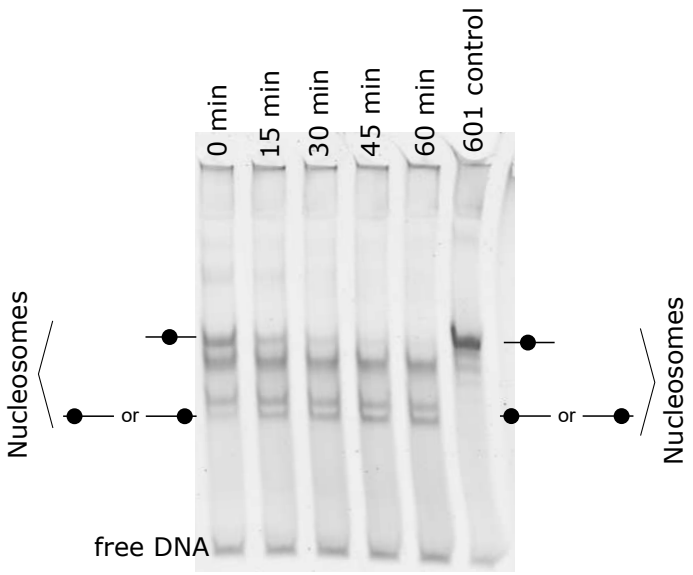

FIG. 5: ISWI-catalyzed nucleosome repositioning of nucleosomes reconstituted with 289 basepairs of random sequence DNA. A control experiment with ISWI-catalyzed repositioning of nucleosomes reconstituted with 289 basepairs of DNA containing the Widom 601 DNA sequence [5] is also shown; the data for this control was collected after 60 minutes of repositioning. Rather than proceeding as a random walk [27], the repositioning of random-DNA-sequence nucleosomes occurs in a single-step reaction.

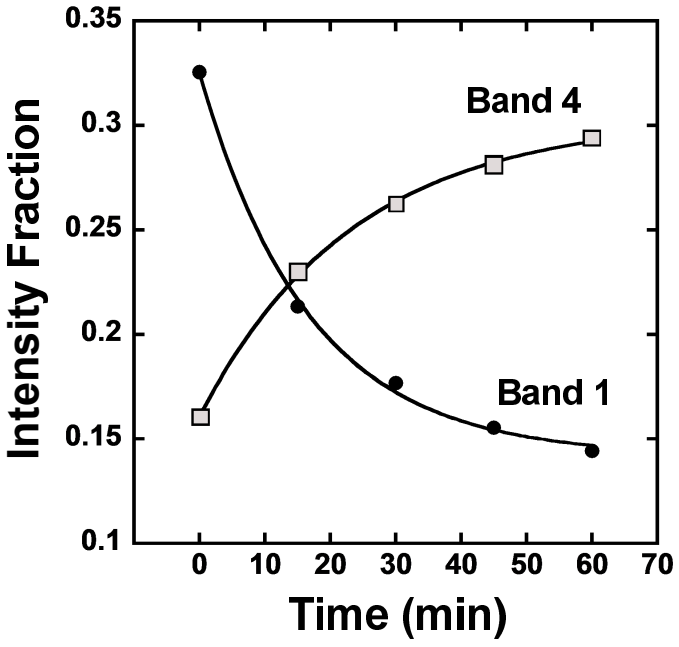

FIG. 6: Analysis of band intensity from ISWI-catalyzed repositioning of nucleosomes reconstituted with random sequence DNA; band 1 (filled circles) corresponds to center positioned NCPs and band 4 (open squares) corresponds to end-positioned NCPs. The average band intensities from three separate experiments are plotted as a function of time following addition of ISWI and ATP. The solid lines are fits of these data to a single-exponential change resulting in rate constants $(0.054 \pm 0.015) min^{-1}$ for band 1 and $(0.074 \pm 0.010) min^{-1}$ for band 2.

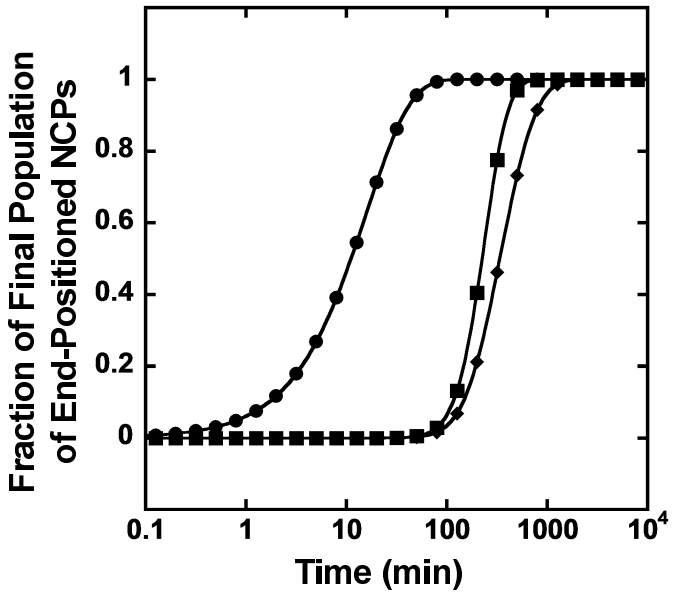

FIG. 7: Simulated time courses of ISWI-catalyzed nucleosome repositioning for different nucleosomes. Nucleosomes reconstituted with random sequence DNA (circles) are repositioned faster than nucleosomes reconstituted with the Widom 601 sequence [5] (squares and diamonds). The two different simulations for repositioning the latter nucleosomes are a random walk model (diamonds) and a sequential n-step model (squares).

repositioning activity observed in Fig. 5 may represent the intrinsic repositioning activity of ISWI. In other words, the rate of repositioning in the experiments shown in Fig. 5 might be limited by the intrinsic ability of ISWI to interact with nucleosomes (both nucleosomal DNA and histone octamers) rather than by the thermodynamics of DNA:histone affinity (see Fig. 4).

It is possible, of course, that the affinity of ISWI binding the NCP is different when the NCP is wrapped with random sequence DNA from when the NCP is wrapped with the Widom 601 sequence containing DNA. Indeed, since remodelers might compete with the histones for DNA binding [32, 33], decreasing the affinity of DNA wrapping within the NCP might increase the affinity of remodeler binding to the NCP. As shown in Fig. 2, decreasing K_D (*i.e.*, decreasing k_d) will shift the observed repositioning reaction from a random walk to a single step process. However, as shown in Fig. 2, changing from a random walk to a single-step reaction would require k_d to change by a factor of $\approx 10^4$, which is far greater than the factor of ≈ 80 estimated from the change in the wrapping energy. Furthermore, since ISWI's affinity for NCP is only a factor of ≈ 10 different from its affinity for binding free DNA, a change in the affinity of NCP binding of a factor of more than $\approx 10^2$ following a change in DNA sequence seems unlikely. Thus, while changes to K_D associated with changing the DNA sequence likely contribute to the observed dependence of observed nucleosome repositioning kinetics on DNA sequence, they are not predominately responsible for it.

We return to the models shown in Fig. 1 and Fig. 3 to offer an explanation based upon kinetic competition for why only a subset of the bands in the gel shown in Fig. 5 appear to be repositioned by ISWI. We begin with the assumption that each band in the gel shown in Fig. 5 corresponds to a nucleosome with the histone octamer at a different position along the DNA. We next assume that the effective rate constant for nucleosome repositioning is different for each of these nucleosomes. This can occur, for example, if the affinity of histone octamer binding varies among the nucleosomes due to variations in DNA sequence (Fig. 4). ISWI will have a higher probability of repositioning nucleosomes with a higher effective rate constant than nucleosomes with a lower effective rate constant; *i.e.*, ISWI will preferentially reposition nucleosomes that present a lower energy barrier to repositioning (Fig. 4). We therefore propose that the energy barrier for repositioning the nucleosomes in band 2 and band 3 is much higher than the energy barrier for repositioning the nucleosomes in band 1 and band 4. Because of this, nucleosomes corresponding to band 1 or 4 are repositioned more quickly than nucleosomes corresponding to band 2 or band 3. This interpretation also suggests that although ISWI can reposition nucleosomes from band 1 (center positioned histone octamers) to band 4 (end positioned nucleosomes), the reserve reaction from band 4 to band 1 does not occur. This could happen, for example, if the processivity of repositioning were so high that ISWI were capable of moving the histone octamers back and forth between the two ends of the DNA. Indeed, since the nucleosomes corresponding to band 4 represent nucleosomes with the histone octamer at either end of the DNA, repositioning of the histone octamer back and forth

between either end of the DNA will not result in a change in the intensity of band 4 in this experiment. Thus, the final dynamic equilibrium of the system involves repeated rounds of ISWI binding to and dissociating from nucleosomes corresponding to band 2, band 3, and band 4, but only repositioning of nucleosomes corresponding to band 4.

A more thorough analysis of ISWI-catalyzed repositioning of NCPs reconstituted with random sequence DNA, including a determination of the NCP structures and positions associated with each band in the EMSA analysis of the repositioning reaction (using restriction enzyme mapping [44, 45], calculations of the affinity of histone binding within each nucleosome, *e.g.*), is beyond the scope and objective of this manuscript. We seek only to demonstrate that the mechanism of ISWI-catalyzed NCP repositioning is indeed influenced by the sequence of nucleosomal DNA, in agreement with the predictions of computer simulations [30] and our mathematical model (Fig. 2).

IV. ASSAY DEPENDENT EFFECTS

Our estimation that at least four fast processes are associated with each slow (*i.e.*, rate-limiting) process for ISWI-catalyzed nucleosome repositioning is consistent with results of single-molecule studies of nucleosome repositioning by ISW2 and ISI1b [24]. In that report, it was proposed that nucleosome repositioning by ISWI-family remodelers proceeds through a coordinated two step process. First, the nucleosome is *primed* for repositioning by the remodeler translocating seven basepairs of DNA (in single basepair increments) to create strain within the wrapped nucleosomal DNA. This strain then allows for an additional three basepairs of DNA to be drawn into the NCP while pushing three basepairs of DNA out of the NCP. This cycle of three basepairs increments of repositioning then repeats until the remodeler dissociates from the nucleosome. While our analysis cannot estimate the rate or number of basepairs of translocated DNA associated with an initiation process prior to processive nucleosome repositioning, our determination that at least four fast processes associated with repositioning (each associated with between 1 and 3 basepairs translocated) is consistent with these observations. Furthermore, the estimate of $(40 \pm 7) min^{-1}$ for DNA translocation reported in these single-molecule experiments [24] is also consistent with the values of k_1 determined for $n \geq 4$ in Table III. These results thus also suggest that the rate of DNA translocation by ISWI is slowed considerably when the DNA is wrapped within (or otherwise in contact with) the NCP than when the DNA is free in solution [41]. This NCP-imposed impairment of ISWI's DNA translocation activity might also account for why the kinetic step-size for DNA translocation also appears to be reduced from 5 basepairs for free DNA [41] to 3 basepairs or fewer for nucleosomal DNA. There was no explicit determination of the rate constant associated with the release of strain within the NCP (and/or associated conformation change in the remodeler) in these single molecule studies [24] with which we can compare our calculation of k_2 (Table I and Table III). Similarly, ATPase rates were not reported for these single-molecule experiments so it is not possible to correlate ATPase rate with repositioning rate as we have done previously [27]. This also prevents a determination of whether a similar high percentage of futile repositioning events occurred. However, since the nucleosomes used in these single-molecule experiments were also reconstituted using DNA containing the Widom 601 sequence [5] we would assume that repositioning would be similarly inefficient. Thus, both the ensemble and single-molecule experiments are likely monitoring a very rare event, occurring $\lesssim 1\%$ of the time a nucleosome is bound by ISWI, whose corresponding rate constants are more likely more indicative of the the thermodynamics of DNA wrapping within the NCP rather than the intrinsic repositioning activity of ISWI.

In order to determine an estimate of the initiation (*i.e.*, nucleosome priming) process indicated by the results of these single-molecule experiments [24], we monitored the repositioning of nucleosomes with shorter lengths of DNA flanking the NCP than we used previously [27]. Specifically, we monitored the ISWI-catalyzed repositioning of 10N24 and 24N24 nucleosomes using the molecular metronome assay [27] (see Materials and Methods). The nomenclature used to designate different nucleosome substrates is xNy where x and y denote the length of DNA flanking the NPS, denoted as "N" [27, 38, 46]; fluorophore labels are denoted as "F". The time dependent increase in anisotropy observed with the 24N24F and 10N24F nucleosomes (Fig. 8) is consistent with ISWI widening the initial distribution of histone octamers to include translational positions on the flanking DNA closer to the fluorophores [27]. The solid lines in Fig. 8 are the results of analysis of these time courses using a random walk model, which returned values of $k_{eff} = (0.026 \pm 0.003) min^{-1}$ for 24N24F and $k_{eff} = (0.023 \pm 0.003) min^{-1}$ for 10N24F, both of which are consistent with previously published results [27]. In contrast, the time dependent decrease in anisotropy observed with the F10N24 nucleosome (Fig. 8) is consistent with ISWI widening the initial distribution of histone octamers to include translational positions on the flanking DNA farther from the fluorophores. In other words, the time course observed for the F10N24 is consistent with ISWI moving the octamer away from the fluorophore. Since the apparent rate constant for this process $(0.12 \pm 0.04) min^{-1}$, determined by fitting the time course of anisotropy to a single-exponential decrease, is much faster than the apparent rate constant for repositioning for this substrate ($\approx 0.025 min^{-1}$), we speculate that it corresponds to a initiation process that proceeds processive nucleosome repositioning. In other words, the repositioning assays with F10N24 and 10N24F are not monitoring the same part of the repositioning mechanism. Additional experiments would be required to disentangle the reason for difference between our estimate of the rate

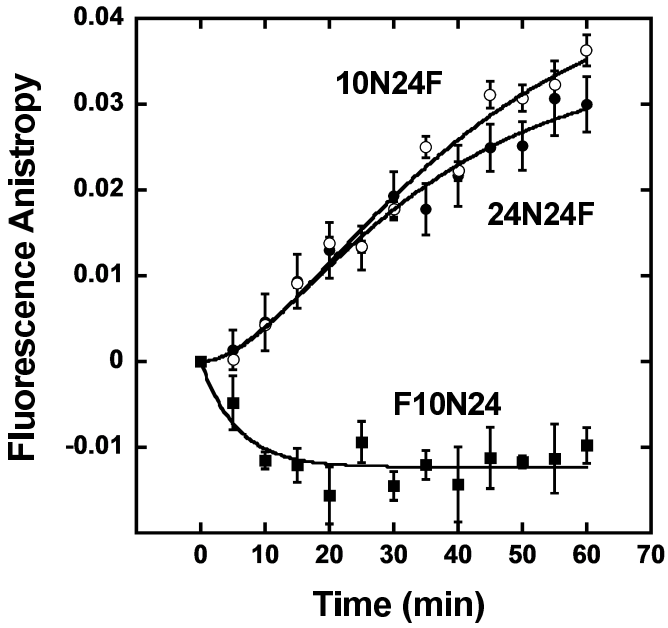

FIG. 8: The ISWI-catalyzed repositioning of nucleosomes monitored through changes in fluorescence anisotropy [27] 24N24F solid circles, 10N24F open circles, F10N24 solid squares. The solid lines are the results of analysis of the data (see text).

constant for repositioning initiation, $(0.12 \pm 0.04)min^{-1}$, and that determined from single-molecule experiments, $(31 \pm 2)min^{-1}$ [24], which may include variations among the different remodelers studied or systematic differences from the assays or substrates employed.

V. EFFECTS OF DNA DAMAGE ON NUCLEOSOME REPOSITIONING

It was proposed recently that the introduction of a DNA lesion changes the energy landscape of a nucleosome such that the new energy minimum of the system corresponds to a different location of the histone octamer on the DNA [47]. Specifically, DNA lesions which increase the rigidity of DNA are more likely to be found in the linker DNA between NCPs whereas lesions that decrease the rigidity of the DNA are more likely to be found at the nucleosome dyad [47]. We propose that these lesion induced changes in the thermodynamics of DNA:histone interactions will alter how nucleosomes are repositioned by chromatin remodelers. Support of this hypothesis is found in studies demonstrating that the rate of nucleosome repositioning by ISWI is enhanced in reactions in which a single nick is repositioned from the linker DNA into the NCP [19]. We can now quantitatively investigate this proposal using this data and Eq. 5.

We first notice that the time course of ISWI-catalyzed nucleosome repositioning reported by Längst *et al.* [19] differs from what we have previously observed [27]. Specifically, in our repositioning time courses the largest population of nucleosomes remained at the center (*i.e.*, initial position on the DNA) [27] whereas in Längst *et al.* the largest populations of nucleosomes are found at the flanking positions on the DNA (*i.e.*, not at the initial position) [19]. Thus, while the former case is consistent with the expectation of a random walk, the latter is a biased random walk [39]. We propose that this difference results from the different DNA sequences used to reconstitute the nucleosomes in these studies. We used the Widom 601 sequence [5] for nucleosome reconstitution [27] and Längst *et al.* used a sequence from the pMrWT plasmid containing the mouse transcription start site [19, 42]. The relative affinities of these sequences for wrapping the histone octamer ($\Delta\Delta E_{sequence}$) is $(2.0 \pm 0.6)k_BT$ [6]. According to Eq. 17, this would correspond a change in k_2 of a factor of 7 ± 4. An increase in k_2 associated with this change in DNA sequence would still leave $k_2 << k_1$ for the parameters shown in Table I and Table III and thus the repositioning reaction would still proceed through the random walk mechanism described by Eq. 4 through Eq. 11. However, this change in DNA wrapping affinity may nevertheless account for the difference in equilibrium distribution of nucleosome states observed in the two sets of experiments.

To further dissect these results, consider the simplified repositioning model shown in Fig. 9. The populations B_{-1},

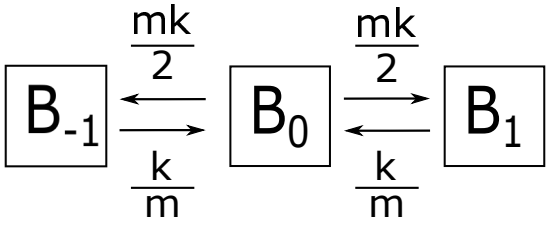

FIG. 9: Simplified three state NCP repositioing model with biased directionality.

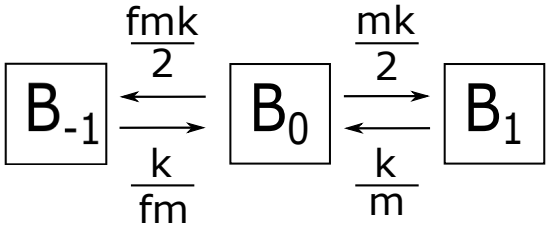

FIG. 10: Three state NCP repositioning model with asymmetric directional bias.

B_0, and B_1 in Fig. 9 denote nucleosomes with octamers at binding position -1, 0, and 1, respectively, on the DNA; position 0 is the center position on the DNA. The effective rate constant for transitions between states in this model is denoted by k and the scalar factor m accounts for modifications of this rate resulting from the thermodynamics of the DNA:histone interactions at the different octamer binding sites, intrinsic bias to the repositioning activity of the remodeler, *etc.* At equilibrium the fraction of the nucleosome populations would be given by Eq. 18.

$$\frac{B_0}{B_{-1}+B_1} = \frac{1}{m^2} \tag{18}$$

A ratio of $\frac{B_0}{B_{-1}+B_1} \approx 0.85$ was reported by Längst *et al.* [19], corresponding to $m \approx 1.08$. Thus, there is a 8% enhancement in repositioning away from the center position on the DNA as opposed to toward that location. Since a change of a factor of ≈ 16 in K_D would be required to shift the repositioning reaction from a pure random walk to this biased random walk [42] (Fig. 2), we believe that this biased random walk results predominately from the intrinsic repositioning activity of ISWI, rather than the affinity of ISWI binding the NCP. An intrinsic ability of ISWI to reposition NCPs towards the end of the DNA is also consistent with ISWI-catalyzed repositioning of nucleosomes reconstituted with random sequence DNA (Fig. 5 and Fig. 6) as well as other studies [42].

Alternatively, it is possible that the kinetics of histone octamer binding are affected by the length of the DNA flanking the histone octamer. Indeed, we have shown previously that ISWI can bind to DNA flanking the histone octamer if the length of the DNA is long enough [38]. In the presence of ATP, ISWI bound to sites on the flanking DNA could translocate along the DNA to subsequently bind the histone octamer. In this way, the affinity of histone octamer binding in the presence of ATP would increase with increasing DNA length; this is different from binding in the absence of ATP for which we have shown no dependence on the length of flanking DNA [38]. If an increase in histone octamer binding (resulting from translocation from initial sites on flanking DNA) did occur, however, we would expect that nucleosomes with longer flanking DNA would be repositioned more quickly than nucleosome with shorter flanking DNA. Since ISWI instead shows a preference for repositioning histone octamers away from the center position on the DNA (*i.e.*, from a nucleosome with symmetric lengths of DNA flanking the histone octamer to a nucleosome with asymmetric lengths - one longer than the other - of DNA flanking the histone octamer), we might conclude that ISWI binding a histone octamer following translocation along the flanking DNA on one side of the histone octamer is binding in an orientation that does not result in repositioning back along the flanking DNA on this side of the histone octamer. Additional experiments are clearly needed to determine the underlying kinetic and/or thermodynamic origin of the directional bias to nucleosome repositioning by ISWI.

Our ability to discern the origin of the directional bias to ISWI-catalzyed nucleosome repositioning does not prevent us from characterizing the effects of DNA damage on this reaction, however. We begin by noting that the inclusion of a single nick in one strand of the DNA flanking the NCP affects the rate of ISWI-catalyzed nucleosome repositioning [19]; in these experiments, the nick was located immediately adjacent to the nucleosome positioning sequence and

thus is immediately outside of the histone octamer in the reconstituted nucleosomes. We can denote the enhancement of the repositioning reaction resulting from the incorporation of this DNA damage using a scalar factor f as shown in Fig. 10. According to this model, the fraction of the nucleosome populations observed at equilibrium would be given by Eq. 19.

$$\frac{B_0}{B_{-1}+B_1} = \frac{2}{m^2(f^2+1)} \tag{19}$$

A ratio of $\frac{B_0}{B_{-1}+B_1} \approx 0.65$ was reported by Längst *et al.* [19] for the repositioning of nucleosomes containing a single nick. Thus, given $m \approx 1.08$, we conclude that $f \approx 1.28$, indicating a 28% enhancement in repositioning of the damaged DNA into the NCP as opposed to into the linker DNA. This enhancement would require a factor of ≈ 50 change in K_D [Fig. 2(b)], which seems unrealistically large. Alternatively, this enhancement is consistent with the fact that the DNA containing a nick is more flexible than undamaged DNA and thus can be wrapped more easily in the NCP [47]. In other words, the presence of the DNA nick has lowered the energy barrier ISWI must overcome to incorporate the damaged DNA into the NCP and thereby enhanced the rate at which ISWI repositions the nicked DNA into the NCP (Fig. 11), perhaps in the form of a loop. Similarly, this same change in DNA flexibility and associated nucleosome thermodynamic stability results in a decrease in the rate of repositioning the NCP such that the nicked DNA is outside of the NCP (and thus un-nicked DNA is wrapped in the NCP). We will assume that the process associated with rate constant k_2 in the model shown in Fig. 1 or Fig. 3 is always energetically rate-limiting for the repositioning reaction regardless of the present of DNA damage; we are therefore assuming that DNA translocation by ISWI is not significantly affected by the presence of a single nick. Based upon the derivation of Eq. 17, we can express the change in k_2 associated with the introduction of damage using Eq. 20

$$\frac{k_{2,A}}{k_{2,B}} = e^{\Delta\Delta E_{damage}} \tag{20}$$

The variable $\Delta\Delta E_{damage}$ in Eq. 20 is related to the change in the thermodynamic stability of the nucleosome (from changes in the affinity of DNA wrapping the NCP, *e.g.*) associated with the introduction of DNA damage. Since the factor $f \approx 1.28$ is equal to the ratio of the value of k_2 for ISWI repositioning nicked DNA into the NCP to the value of k_2 for ISWI repositioning undamaged DNA into the NCP, Eq. 20 predicts a value of $\Delta\Delta E_{damage} = -0.24 k_B T$.

The energy associated with bending DNA of length l over an angle θ is shown in Eq. 21 [48].

$$E_{wrap} = \frac{k_B T l_p}{2l}\theta^2 \tag{21}$$

The variable l_p in Eq. 21 is the persistence length of the DNA. For single-stranded DNA, $l_{p,ss} = (0.68 \pm 0.07) nm$ [49–51], and for double-stranded DNA $l_{p,ds} = (60 \pm 5) nm$ [52–54]. The central 129 basepairs of DNA within the nucleosome are wrapped 1.59 turns around the histone octamer [1, 3]; the 10 basepairs of DNA at each terminus of the NCP are essential unbent [1]. Thus, the total angle for the DNA wrapping is $1.59(2\pi)$=10 *rad.* Finally, the length of wrapped DNA depends upon the radius of curvature of the DNA in the nucleosome, 4.2 *nm* [1, 3], and is $l = (4.2\ nm)(10\ rad) = 42\ nm$. Thus, the total energy of wrapping the DNA within the nucleosome is

$$E_{wrap,ds} = \frac{k_B T((60\pm5)nm)}{2(42nm)}(10rad)^2 = (71 \pm 6) k_B T$$

$$E_{wrap,ss} = \frac{k_B T((1.6\pm0.6)nm)}{2(42nm)}(10rad)^2 = (0.81 \pm 0.08) k_B T$$

Since there are 14 electrostatic contact points between the octamer and the nucleosomal DNA in the NCP, there are 13 regions of wrapped DNA in the NCP [1]; each region is $129/13 = 9.9$ *bp* long. Thus, the wrapping energies per wrapped region are $(5.5\pm0.5) k_B T$ and $(0.062\pm0.006) k_B T$ for double-stranded and single-stranded DNA, respectively. A first order approximation of the wrapping energy for a region of DNA containing a single nick would be

$$E_{wrap,nicked} = \frac{9E_{wrap,ds}+E_{wrap,ss}}{10} = (5.0 \pm 0.5) k_B T$$

Therefore, the reduction in wrapping energy following the introduction of a single nick is $(5.0 \pm 0.5) k_B T - (5.5 \pm 0.5) k_B T = -(0.5 \pm 0.7) k_B T$. This result is within the uncertainty of the estimated change in energy determined from the change in the rate of repositioning and thus is consistent with the hypothesis that changes in the thermodynamics of histone:DNA interactions affects the rate of remodeler-catalyzed nucleosome repositioning. Interestingly, this results

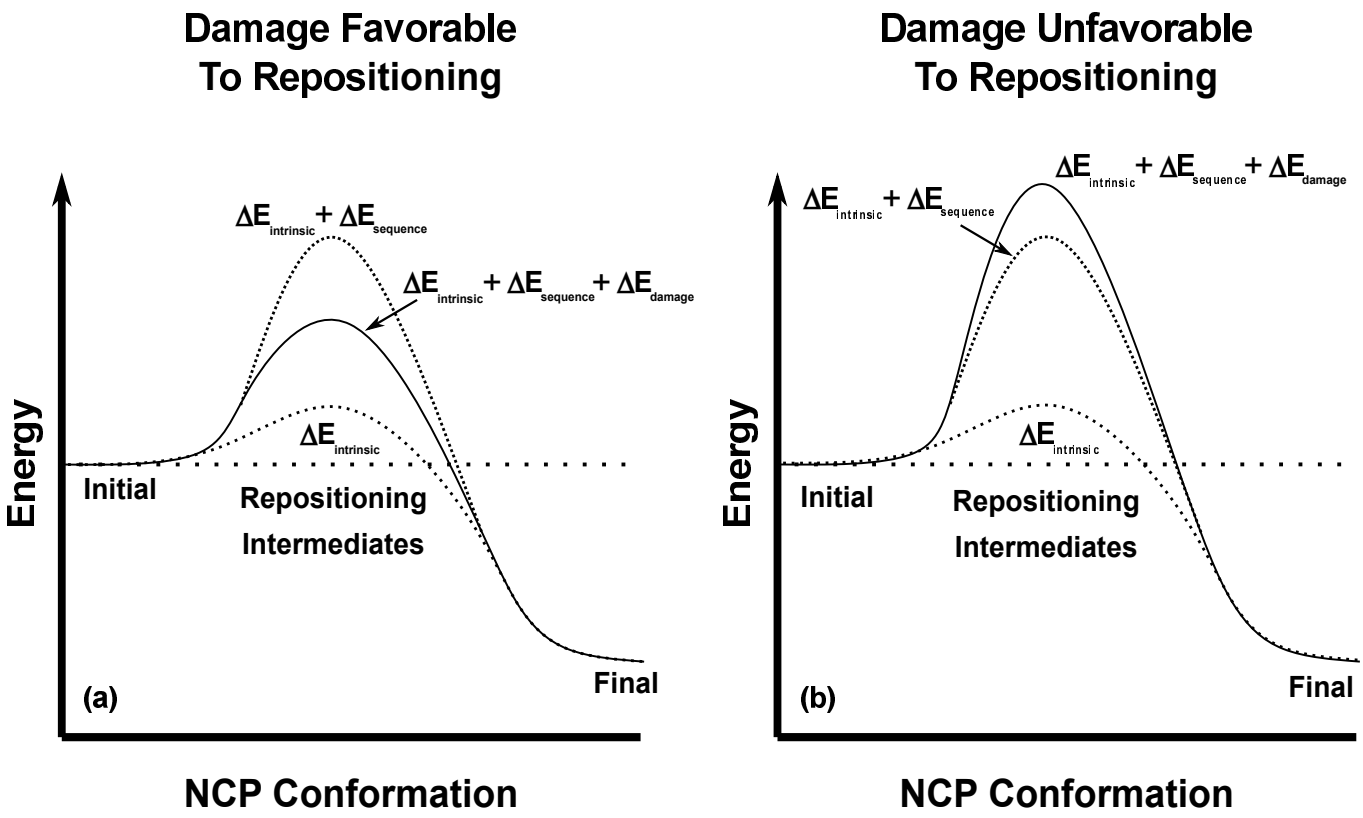

FIG. 11: The energy barrier to repositioning is a sum of contributions from the intrinsic energy barrier ($\Delta E_{intrinsic}$) associated with the biophysics of the remodeler interaction with the nucleosome, a DNA sequence specific energy barrier ($\Delta E_{sequence}$) related to DNA sequence changes to NCP stability, and changes in histone:DNA or remodeler:DNA interactions associated with DNA damage (ΔE_{damage}). ΔE_{damage} can lower (a) or raise (b) the energetic barrier to repositioning depending upon its type and location [47] and thus can be favorable or unfavorable to nucleosome repositioning.

also suggests that rather than assuming the nick introduces 10% single-stranded 'character' into the energetics of the DNA, the nick introduces closer to 5%. Längst *et al.* did not report the ATPase activity of ISWI when repositioning the single nick containing nucleosome [19], but we would anticipate that the ATPase rate would differ by less than 28% since it is dominated by the fraction of nucleosome-bound ISWI, which, as mentioned previously, is likely unaffected by the introduction of the nick.

VI. CONCLUSION

The sequence of nucleosomal DNA has been shown to influence the nucleosome repositioning activity of chromatin remodelers [26–30], likely due to the DNA sequence dependence of the interactions between the remodeler and the nucleosome, between the remodeler and the DNA, and/or between the DNA and the histones. Indeed, it is well known that the affinity of DNA wrapping within the NCP is determined by the sequence of nucleosomal DNA [5–7, 12]. Here we have shown that variations in the affinity of DNA wrapping within an NCP can also affect the rate of ISWI-catalyzed nucleosome repositioning and can even shift the repositioning reaction from proceeding as a random walk to a single step process. Thus, determining the microscopic and macroscopic parameters associated with mechanisms of remodeler-catalzyed nucleosome repositioning requires a quantitative characterization of the affinity of all interactions between the remodeler, the DNA, and the histone octamer. This includes, of course, characterizing the stoichiometry with which the remodeler binds the NCP [38] so that the active oligomeric state of the remodeler can be identified [27].

A. NCP Stability Modulates ISWI Function

We have demonstrated that the ISWI-catalyzed repositioning of nucleosomes reconstituted with the DNA containing the Widom 601 sequence [5, 27] is energetically limited by a process other than DNA translocation; nevertheless these results suggest that DNA translocation by ISWI (both macroscopic rate and kinetic step-size) are impaired when the DNA is wrapped within the NCP. We propose that this energetically limiting process is associated with the breaking and re-establishing of histone:DNA contacts and/or other associated changes in the topology of the DNA (such as bending the DNA or propagating a loop of DNA around the NCP) and is therefore dependent upon the thermodynamic stability of the NCP (the energy required to bend the DNA, *e.g.*). In experiments conducted with nucleosomes reconstituted with DNA containing the Widom 601 sequence, between 99% and 99.9% of all ISWI:nucleosome binding events result in futile repositioning, in which ATP hydrolysis but no movement of the NCP occur; this model is thus consistent with the poor ATP coupling efficiency reported for ISWI repositioning these nucleosomes [27]. We argue that the thermodynamic stability of DNA wrapping within the NCP of these nucleosomes (*i.e.*, the high affinity of the DNA for wrapping within the NCP) strongly impairs the ability of ISWI to successfully reposition the NCP by decreasing the ability of ISWI to compete with the histones for DNA binding. Consequently, the rate constants determined for ISWI-catalyzed repositioning of these nucleosomes (Table I and Table III) reflect more strongly the thermodynamics of the interactions between the histones and the DNA within the NCP rather than the intrinsic repositioning activity of ISWI itself. This result is also manifest in the ISWI-catalyzed repositioning of nucleosomes reconstituted with random sequence DNA (Fig. 5). Changing the sequence of nucleosomal DNA from containing the Widom 601 sequence to containing random sequence DNA can shift the rate of nucleosome repositioning by a factor of at least 20 while simultaneously changing the mechanism from a random walk to a single step process. Thus, we believe that the rate of repositioning observed in the experiments shown in Fig. 5 more accurately correspond to the intrinsic NCP repositioning activity of ISWI.

Our estimate of $(0.12 \pm 0.04) min^{-1}$ for the process by which ISWI initiates the repositioning reaction is about two orders of magnitude slower than that measured in the single-molecule studies ($(31 \pm 2) min^{-1}$)[24]. This difference in rates may reflect differences in the mechanisms of repositioning between the different remodelers used in these studies (*i.e.*, ISWI [27] *vs.* ISW2 and ISW1b [24]), but this seems unlikely given the apparent similarity in their rates of DNA translocation (Table III). The difference in rates may result from changes in the affinity of the remodeler to bind nucleosomes having a short piece of flanking DNA on one side of the NCP [24], but no effect of the length of flanking DNA was observed in previous studies of nucleosome binding by ISWI [27]. Lastly, it is possible that the repositioning initiation process (or other processes, such as those associated with k_2 in the models in Fig. 1 and Fig. 3 or initial rounds of DNA translocation) are enhanced by having a short length of linker DNA flanking the NCP [24]. Indeed, these results suggest that shortening the length of the linker DNA flanking the NCP increases the rate of the initiation process proceeding processive repositioning without affecting the affinity of NCP binding by the remodeler. If so, this phenomenon can reconcile why some previous studies of nucleosome repositioning reported no dependence upon DNA sequence [55] whereas other studies reported a strong dependence [26–29]. Specifically, the former experiments may have monitored an initiation process whose rate was dominated by the short length of linker DNA rather than any DNA sequence contributions. This suggests that experiments monitoring the repositioning of nucleosomes reconstituted with very short flanking DNA, as is common for several FRET based assays [24, 55–58], may be over-estimating this initiation rate. More significantly, if this initiation process is not rate-limiting for the repositioning reaction, as our data suggest, the inherent experimental bias in these assays might mask differences in the repositioning mechanism associated with perturbations of the system (change in NPS, post-translational modifications, *etc.*).

B. DNA Damage Can Facilitate Its Own Detection

Changes in DNA rigidity resulting in DNA wrapping becoming more or less favorable, such as a change in DNA sequence [30] or the introduction of a DNA lesion [47], should affect the repositioning reaction. A decrease in the affinity of DNA wrapping within the NCP can result in an increase in the affinity of NCP binding by the remodeler (*i.e.*, a shift in the competition between the remodeler and histones for binding the DNA [32]), which will increase the processivity of repositioning by the remodeler (Fig. 2). Alternatively, a decrease in the affinity of DNA wrapping within the NCP can lower the energy barrier to repositioning. For example, the rate of nucleosome repositioning by ISWI is enhanced in reactions in which a single nick is repositioned from the linker DNA into the NCP [19]. As we have demonstrated, this enhancement in the rate correlates well with the reduction of the energy required for wrapping the damaged DNA within the NCP. We would similarly expect that DNA lesions that increase the rigidity of DNA would be more easily moved from the NCP to the linker DNA. Support for this proposition has also already been observed. One of the major forms of DNA damage caused by overexposure to UV radiation is the (6-4) pyrimidine-pyrimidone

adduct [59], which increases the rigidity of the DNA [60, 61]. As anticipated, (6-4) pyrimidine-pyrimidone adducts are 6-fold more likely to be found in linker DNA than in the NCP [62]. In this way, DNA damaged induced changes to NCP thermodynamics can influence chromatin remodeler activity resulting in a targeted relocation of DNA damage. It is also possible, of course, that the DNA-sequence changes to the thermodynamics of DNA wrapping within the NCP may facilitate remodeler-independent transitions of the NCP to different positions on the DNA [47]. An analysis of the temperature dependence of nucleosome repositioning in the presence and absence of remodelers is required to determine the fraction of the energy barrier to repositioning reduced by changes in DNA wrapping dynamics.

This self-reorganization of DNA damage would naturally affect the rate of DNA damage detection since it would remove the necessity to search all of the cell's DNA by concentrating the damage at locations where it is more likely to be found. In agreement with this proposition are examples of DNA damage detection proteins that preferentially bind nucleosomal DNA at the dyad [63] or in regions of increased DNA flexibility, such as in the linker DNA [64]. The efficiency of these proteins to detect their targets would be increased if nucleosomes were capable of adjusting themselves to place these damage targets in these preferred binding locations. Indeed, the ability of DNA damage to self-organize within a cell would minimize the accumulation of permanent damage to the cell's genetic material, constituting a significant evolutionary advantage for eukaryotes.

C. Coupling Between NCP Stability and Chromatin Remodeler Function

The dependence of the mechanism of nucleosome repositioning on the thermodynamics of the interactions between the remodeler, the nucleosomal DNA, and the histones demonstrates the necessity of independently and quantitatively characterizing each of these interactions to accurately model the repositioning reaction [26, 27, 38]. In the absence of such information, one cannot be certain that the measured time courses of nucleosome repositioning are reporting on the affinity of the remodeler to bind the NCP, the affinity of the DNA for wrapping within the NCP, *e.g.*, rather than on the intrinsic activity of the remodeler itself, including potential initiation processes [24]. Indeed, it is likely that post-translational modification of histones and/or chromatin remodelers affect nucleosome repositioning [16, 18] by modulating the affinity of interactions between the remodeler, the histones, and the nucleosomal DNA. For example, the sensitivity of ISWI's nucleosome repositioning activity to modifications within the H4 tail [65, 66] may suggest that these modifications regulate the affinity of ISWI binding to the NCP; for example, the human ISWI homolog Snf2 is known to interact directly with the H4 tail when bound to an NCP [33]. This would not be surprising as the dynamics of residues within the H4 tail are known to change when the NCP is bound by remodelers, including SNF2H [34]. The energetics associated with histone distortion following remodeler binding [34] could easily be modulated by post-translational modifications of the histones, particularly the H4 tail, and therefore the thermodynamics (affinity, *e.g.*) of remodeler binding could also be modulated by these same histone modifications. Similarly, both the affinity of NCP binding and the rate of NCP repositioning by ISWI are increased in the presence of histone variant H2A.Z [67]. These observations may well be coupled such that the increase in the repositioning rate is a simple consequence of ISWI remaining bound longer to the NCP in the presence of H2A.Z. Indeed, as we have shown here, variations in the affinity with which the remodeler binds the NCP and/or the DNA wraps the NCP can affect the mechanism and associated rates of nucleosome repositioning. These effects are, of course, not limited to ISWI family chromatin remodelers. Acetylation of the H3 tail has been shown to increase both the affinity of NCP binding and the rate of NCP repositioning by the SWI/SNF and RSC chromatin remodelers [68]. This stimulation of the NCP repositioning rate was not concomitant with an increase in the ATP hydrolysis rate, suggesting that H3 tail acetylation is reducing the amount of futile repositioning (and associated futile ATP hydrolysis) occurring in the reaction. This is exactly what is predicted from the models (Fig. 2) if k_d decreases (*i.e.*, K_D decreases). Since acetylation of histone tails does not affect the affinity of DNA wrapping within the NCP [69, 70], the change in NCP binding affinity associated with the acetylation of histone tails suggests a direct interaction between the remodeler and the tails, as has been previously reported [71–74]. Finally, the enhancement of NCP stability resulting from the 5-formylcytosine modification of nucleosomal DNA could explain the enrichment of this modification at the transcription start sites of low-expression genes [8]. Specifically, it is this DNA modification that results in the low expression of these genes by limiting the ability of transcription machinery, including chromatin remodelers, to reposition the NCPs.

D. Implications for Repositioning Mechanism

Our data are consistent with a model in which nucleosome repositioning occurs through two ATP-coupled processes. The faster of these two processes, which we have tentatively associated with DNA translocation, involves the cyclic repeat of at least 4 steps, each associated with the binding and hydrolysis of a single ATP molecule. We associate the slower process, which is energetically rate limiting for the entire repositioning reaction, with the energy required

to change the topology of the DNA within the NCP (to unwrap and rewrap the DNA) or the breaking of contacts between the histones and the DNA, or a combination of these operations. If the remodeler fails to complete either of these two processes before it dissociates from the NCP, the NCP is reset to its previous configuration. This model is consistent with the proposal that ISWI's two RecA-like core domains [75] form a tracking element that remains fixed to the NCP, likely through direct contacts with the histones [33, 34], and a torsion element that translocates along the nucleosomal DNA [33]. Dissociation of the moving torsion element before completing the energetically rate-limiting process would account for the observed poor coupling efficiency of ATP binding and hydrolysis to NCP repositioning. Indeed, if the the tracking element remains bound to the NCP, then multiple rounds of futile repositioning (repeated cycles of translocation and dissociation of the torsion element) could be associated with each binding of the remodeler to the nucleosome. Our results cannot directly distinguish between an inchworm loop-propagation model, where DNA loops are introduced on one side of the NCP and move around the histone octamer to the other side of the NCP, and a twist diffusion model, in which a defect in DNA helicity is introduced and then diffuses around the NCP in a corkscrew manner. However, the similarity between the 10 basepair increments observed for ISWI-catalyzed nucleosome repositioning [27] and the pitch of the DNA is consistent with the expectations of a twist diffusion model [30].

It is worth noting that coarse grain molecular modeling of NCP dynamics suggest that DNA loops occurring for a inchworm loop-propagation model are unevenly distributed along the surface of the NCP, and concentrated at SHL$\pm$2 [30]. When combined with observations that Snf2 binds preferentially to the NCP at SHL2 [33], these results support a proposed step-wise molecular ratchet model where a DNA loop is pulled into the NCP and localized at SHL$\pm$2, moved across the NCP (perhaps being pulled by the H4 tail at SHL$\mp$2), and then released from the other side of the NCP [30]. The fast and slow processes associated with our model would then correspond to the loop formation (through DNA translocation, *e.g.*) and loop propagation processes, respectively. Consistent with this model is our observation that failure to complete the slow process results in resetting of the nucleosome to its original configuration, perhaps through the expulsion of the initial loop from the NCP. Measurements of the kinetic parameters for ISWI-catalyzed repositioning of NCPs reconstituted with different sequences of DNA are required to resolve this mechanism further.

Recently published structures of chromatin remodelers bound to their NCP substrates have provided invaluable snapshots into the function of these essential machines and caution about how to interpret the results of other experiments. For example, structures determined from cryo-electron microscopy revealed two binding sites for Snf2 on an NCP [33], one at SHL2 and the other at SHL6 where interaction with the linking DNA is possible; a small fraction of NCPs were detected bound with two separate Snf2 remodelers, one at each of these sites. The presence of multiple chromatin remodeler binding sites on an NCP will naturally complicate the interpretation of peptide mapping experiments [76, 77] seeking to determine how remodelers interact with NCPs and mechanistic models for nucleosome respositioning derived therefrom. Similarly, our results presented here demonstrate the necessity of independently characterizing both the affinity of DNA wrapping within the NCP (*i.e.*, NCP stability) and the affinity and stoichiometry of NCP binding by the remodeler to model correctly the kinetics of remodeler-catalyzed nucleosome repositioning and its dependence upon DNA sequence, post-translational modifications, variations in histone content, *etc.*. Specifically, both the movement of the NCP and the rate of ATP hydrolysis by the remodeler are necessary to determine the corresponding kinetic parameters for this modeling [27, 38]. We have shown that a global analysis of both the ATPase and NCP movement rates can distinguish which processes are energetically rate-limiting for the respositioning reaction. More broadly, we propose that at least some of the diversity of chromatin remodeler behavior (influence of DNA sequence, influence of post-translational modifications of histones, preferences in NCP positioning, *etc.*) are an emergent property of modulations within the network of interactions between histones, nucleosomal DNA, and chromatin remodelers and/or can be strongly influenced by the assay used to monitor the activity of the remodeler. Accordingly, deconvoluting the intrinsic activity of the remodeler requires simultaneous analysis of different assays for NCP binding and repositioning (NCP movement, remodeler ATPase, *e.g.*) using nucleosomes reconstituted with different DNA sequences, including those with low affinity for wrapping the NCP, and being aware of (and possibly correcting for) any systematic biases in the experiments used to monitor these remodeler activities. Only through a combined approach can one correctly describe not only remodeler function, but also how DNA sequence, post-translational modifications, interaction with other regulatory proteins within or outside of the chromatin remodeling complex, *etc.*, affect this function.

VII. MATERIALS AND METHODS

Protein Expression and Nucleosome Reconstitution: *Xenopus Laevis* ISWI, histones H2A, H2B, H3 and H4 were expressed and purified according to previously published protocols [27, 38]. DNA fragments containing the 148 bp 601 high affinity nucleosome positioning sequence [5] (Sequence-containing plasmid is a kind gift from Timothy J. Richmond) and additional length of flanking DNA was amplified using large scale PCR followed by purification of

the amplified fragment. The 601 sequence consisted of the following sequence:
CGGG ATCC TAAT GACC AAGG AAAG CATG ATTC TTCA CACC GAGT TCAT CCCT TATG TGAT GGAC CCTA TACG CGGC CGCC CTGG AGAA TCCC GGTG CCGA GGCC GCTC AATT GGTC GTAG ACAG CTCT AGCA CCGC TTAA ACGC ACGT ACGC GCTG TCCC CCGC GTTT TAAC CGCC AAGG GGAT TACT CCCT AGTC TCCA GGCA CGTG TCAG ATAT ATAC ATCC TGTG CATG TATT GAAC AGCG ACCT TGCC GGTG CCAG TCGG ATAG TGTT CCGA GCTC CC
Random sequence DNA was amplified from this same plasmid and consisted of the following sequence:
ACTC TAGA GGAT CCCC GGGT ACCG AGCT CGAA TTCG CCCT ATAG TGAG TCGT ATTA CAAT TCAC TGGC CGTC GTTT TACA ACGT CGTG ACTG GGAA AACC CTGG CGTT ACCC AACT TAAT CGCC TTGC AGCA CATC CCCC TTTC GCCA GCTG GCGT AATA GCGA AGAG GCCC GCAC CGAT CGCC CTTC CCAA CAGT TGCG CAGC CTGA ATGG CGAA TGGC GCCT GATG CGGT ATTT TCTC CTTA CGCA TCTG TGCG GTAT TTCA CACC GCAT ATGG TGCA CTCT CAGT A

Nucleosomes were reconstituted according to previously published protocols [27, 38] using either non-labeled primers or Alexa488 end-labeled primers (IDT, Coralville IA) and were evaluated using a 5% native polyacrylamide-bisacrylamide gel (60:1) run at 100 V in 0.25x Tris-Borate-EDTA (TBE) buffer followed by either staining using SYBR® gold or exposed for fluorescence and imaging using a Typhoon imager (GE Healthcare).

Gel based repositioning assays: 10 nM ISWI was incubated with 50 nM nucleosome substrates in reaction buffer (10 mM HEPES (pH 7.0), 20 mM KCl, 10 mM MgCl2, 4% glycerol, 0.1 mg/ml BSA, 0.5 mM DTT) at 25 °C. Repositioning reactions were initiated by the addition of 1 mM ATP and allowed to proceed for specific time points before stopping by the addition of quenching solution containing EDTA and competitor plasmid DNA. The reactions were then analyzed using 5% native polyacrylamide-bisacrylamide gel (60:1) run at 100 V in 0.25x TBE buffer followed by staining using either SYBR gold and visualized using a Typhoon imager (GE healthcare).

Anisotropy based repositioning assays: ISWI (20 nM concentration) was incubated with 10 nM of Alexa488 labeled nucleosome substrates in reaction buffer (10 mM HEPES (pH 7.0), 20 mM KCl, 10 mM MgCl2, 4% glycerol, 0.1 mg/ml BSA, 0.5 mM DTT) at 25 °C. Reactions were initiated by the addition of 1 mM ATP and the movement of the octamer was detected by monitoring changes in the fluorescence anisotropy of the fluorophore using a Syergy2 fluorescence spectrophotometer (BioTek) set at 485 nm excitation and monitoring emission at 520 nm [27].

Monte Carlo Simulations: All Monte Carlo simulations were programmed with Python 3.6 using Spyder 3.2.3 IDE. Simulations create bins for each state population (B_{0R}, B_{0L}, U_0, U_1, *etc.*) including intermediate states, then loop through each member of each bin once per time-step, checking against assigned probabilities to determine how the populations change according to Fig. 1 and Fig. 3. Checking against probabilities is done through random number generation using Python's 'random.uniform()' function. Populations for time courses are defined by combining each major state population (*i.e.*, $B_{0R} + B_{0L} + U_0$) with the populations of the intermediate states which collapse to that major state upon dissociation (*i.e.*, $B_{0R,1-9}$). Each transition also includes the hydrolysis of a single ATP molecule (*i.e.*, production of a single ADP molecule), which is used to establish an ATP hydrolysis time course.

Data Analysis: Analysis of repositioning and ATPase time courses was performed using R [78]. Cited errors are the standard error of the parameter determined using the nonlinear least squares (nls) algorithm. The average number of steps completed before dissociation in a sequential n-step mechanism is determined using Eq. 22 [43].

$$N_{trans} = \frac{k_1 + k_d}{k_d} \tag{22}$$

VIII. ACKNOWLEDGMENTS

The authors would like to thank Dr. John Karanicolas and Dr. Alexander Moise (University of Kansas) for generous donation of equipment and reagents. We are grateful to Dr. Bradley Cairns (University of Utah) for the histone expression plasmids. We would also like to thank Dr. Timothy J. Richmond (ETH-Zurich) for the kind gift of the nucleosome positioning sequence. We are thankful to Dr. Paul Wade (NIH) for xISWI cDNA.

This work was supported by National Institutes of Health Grants P20 RR017708 and P20 GM103418, a Kansas City Area Life Sciences Institute Patton Trust Grant, and University of Kansas General Research Fund to C.J.F.

IX. APPENDIX

The derivations for equations describing the time dependent populations of nucleosomes repositioned through a random walk were presented previously by Al-Ani *et al.* [27]; we note that Equation A24 in that publication is incorrect. We have followed a similar derivation here to obtain Eq. 1 through Eq. 11.

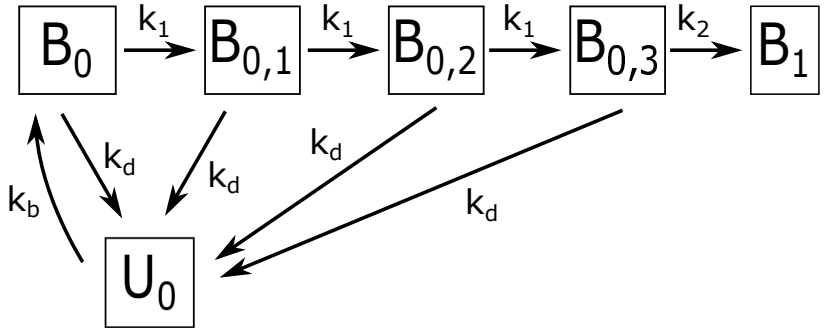

FIG. 12: A simple repositioning reaction involving 3 occurrences of a process associated with a rate constant k_1 and a single occurrence of a process associated with rate constant k_2. The variables k_d and k_b denote the microscopic dissociation and binding constants, respectively, for a remodeler interacting with the nucleosome.

We begin our modification of that derivation by considering the simple model shown in Fig. 12. In this model, a unidirectional repositioning reaction takes a nucleosome from an initial position (denoted as 0) to a final position (denoted as 1) through 3 occurrences of a process associated with rate constant k_1 and a single process associated with rate constant k_2. As before, the populations B_x denote a nucleosome bound by a remodeler with the subscript x denoting the position of the octamer on the DNA. The population U_0 denotes a nucleosome with the octamer at position 0 that is not bound by a remodeler. The differential equations describing the populations in this model are shown below.

$$\begin{aligned}
\tfrac{dU_0}{dt} &= -k_b U_0 + k_d(B_0 + B_{0,1} + B_{0,2} + B_{0,3}) \\
\tfrac{dB_0}{dt} &= k_b U_0 - (k_1 + k_d)B_0 \\
\tfrac{dB_{0,1}}{dt} &= k_1 B_0 - (k_1 + k_d)B_{0,1} \\
\tfrac{dB_{0,2}}{dt} &= k_1 B_{0,1} - (k_1 + k_d)B_{0,2} \\
\tfrac{dB_{0,3}}{dt} &= k_1 B_{0,2} - (k_2 + k_d)B_{0,3} \\
\tfrac{dB_1}{dt} &= k_2 B_{0,3}
\end{aligned}$$

Furthermore, if the total number of nucleosomes in the reaction is denoted as N we can relate all nucleosome populations using Eq. 23.

$$N = U_0 + B_0 + B_{0,1} + B_{0,2} + B_{0,3} + B_1 \tag{23}$$

When either the process associated with k_1 or the process associated with k_2 is rate-limiting, the population B_1 will increase according to a single-exponential; we can equivalently say that the population $B_{0,3}$ will decrease according to a single-exponential. When this occurs, all populations other than B_1 are in dynamic equilibrium with one another and therefore and all of the associate derivatives of those populations with respect to time are zero. Let's focus on the first differential equation shown above.

$$0 = -k_b U_0 + k_d(B_0 + B_{0,1} + B_{0,2} + B_{0,3})$$

Solving for U_0 gives us

$$B_0 + B_{0,1} + B_{0,2} + B_{0,3} = \frac{k_b}{k_d} U_0 \tag{24}$$

Substitution of Eq. 24 into the Eq. 23 gives us

$$N = U_0 + \tfrac{k_b}{k_d} U_0 + B_1$$

$$N = (\tfrac{k_d + k_b}{k_d}) U_0 + B_1$$

Since the variable N is a constant, differentiation of this equation with respect to time gives us the following expression:

$$0 = (\tfrac{k_d+k_b}{k_d})\tfrac{dU_0}{dt} + \tfrac{dB_1}{dt}$$

Which we can further simplify to Eq. 25.

$$0 = \Big(\frac{k_d + k_b}{k_d}\Big)\frac{dU_0}{dt} + k_2 B_{0,3} \tag{25}$$

Now let's return to the remaining algebraic equations describing the relationships between the populations in Fig. 12 when the system is in dynamic equilibrium.

$$\begin{gathered} 0 = k_b U_0 - (k_1 + k_d)B_0 \\ 0 = k_1 B_0 - (k_1 + k_d)B_{0,1} \\ 0 = k_1 B_{0,1} - (k_1 + k_d)B_{0,2} \\ 0 = k_1 B_{0,2} - (k_2 + k_d)B_{0,3} \end{gathered}$$

We can combine these equations to determine the relationship between U_0 and $B_{0,3}$.

$$B_{0,3} = \tfrac{k_b}{k_2+k_d}\big(\tfrac{k_1}{k_1+k_d}\big)^3 U_0$$

Differentiation of this equation with respect to time then yields

$$\frac{dB_{0,3}}{dt} = \frac{k_b}{k_2 + k_d}\left(\frac{k_1}{k_1 + k_d}\right)^3 \frac{dU_0}{dt} \tag{26}$$

Combining Eq. 25 and Eq. 26 gives us a differential equation involving only $B_{0,3}$.

$$\tfrac{dB_{0,3}}{dt} = \tfrac{k_b}{k_2+k_d}\left(\tfrac{k_1}{k_1+k_d}\right)^3 (-\tfrac{k_2}{\frac{k_d+k_b}{k_d}} B_{0,3})$$

Further simplification of this equation yields our final result.

$$\frac{dB_{0,3}}{dt} = \left(\frac{k_b}{k_b + k_d}\Big(\frac{k_1}{k_1 + k_d}\Big)^3 \frac{k_2 k_d}{k_d + k_2}\right) B_{0,3} \tag{27}$$

The solution to Eq. 27 is

$$B_{0,3}(t) = B_{0,3}(t=0)e^{k_{eff}t}$$

As expected, the time evolution of $B_{0,3}$ or equivalently B_1 can be described by a single exponential. The rate constant for this exponential (which is thus the effective rate constant for the repositioning reaction) is given in Eq. 28.

$$k_{eff} = \Big(\frac{k_b}{k_b + k_d}\Big)\Big(\frac{k_1}{k_1 + k_d}\Big)^3\Big(\frac{k_2 k_d}{k_d + k_2}\Big) \tag{28}$$

The first term in Eq. 28 can be simplified using Eq. 1.

$$k_{eff} = \Big(\frac{[R]}{[R] + K_D}\Big)\Big(\frac{k_1}{k_1 + k_d}\Big)^3\Big(\frac{k_2 k_d}{k_d + k_2}\Big) \tag{29}$$

There are two limiting cases for the final term in parenthesis in Eq. 29. When k_2 is large compared to k_d (*i.e.*, when k_2 is not rate-limiting) we have

$$\lim_{k_2 > k_d} \frac{k_2 k_d}{k_d + k_2} = k_d$$

Alternatively, when k_2 is small compared to k_d (*i.e.*, when k_2 is rate-limiting) we have

$$\lim_{k_2<k_d} \frac{k_2 k_d}{k_d + k_2} = k_2$$

We thus have two effective rate constants for the repositioning reaction.

$$k_{eff,1} = \Big(\tfrac{[R]}{[R]+K_D}\Big)\Big(\tfrac{k_1}{k_1+k_d}\Big)^3 k_d$$

$$k_{eff,2} = \Big(\tfrac{[R]}{[R]+K_D}\Big)\Big(\tfrac{k_1}{k_1+k_d}\Big)^3 k_2$$

By extension of these results, we see that the effective rate constants for a system consisting of n occurences of the process assocaited wtih rate constant k_1 would be given by Eq. 30 and Eq. 31.

$$k_{eff,1} = \Big(\frac{[R]}{[R]+K_D}\Big)\Big(\frac{k_1}{k_1+k_d}\Big)^n k_d \tag{30}$$

$$k_{eff,2} = \Big(\frac{[R]}{[R]+K_D}\Big)\Big(\frac{k_1}{k_1+k_d}\Big)^n k_2 \tag{31}$$

Eq. 30 and Eq. 31 are identical to Eq. 2 and Eq. 3.

We can follow a similar approach to determine the equation for the ATPase associated with nucleosome repositioning. Let's assume that each process associated with the rate constant k_1 and the process associated with k_2 will each be associated with the production of a single ADP molecule (*i.e.*, the hydrolysis of a single ATP molecule). Following these assumptions, the differential equation for the concentration of ADP associated with the model in Fig. 12 is shown in Eq. 32.

$$\frac{d[ADP]}{dt} = k_1\big(B_0 + B_{0,1} + B_{0,2}\big) + k_2 B_{0,3} \tag{32}$$

We can then substitute Eq. 24 into Eq. 32.

$$\tfrac{d[ADP]}{dt} = k_1\big(\tfrac{k_b}{k_d}U_0 - B_{0,3}\big) + k_2 B_{0,3}$$

$$\tfrac{d[ADP]}{dt} = k_1\Big(\tfrac{k_b}{k_d}\Big)U_0 + (k_2 - k_1)B_{0,3}$$

Then we express $B_{0,3}$ in terms of B_0 using the same approach described above.

$$\frac{d[ADP]}{dt} = k_1\Big(\frac{k_b}{k_d}\Big)U_0 + (k_2 - k_1)\Big(\frac{k_1}{k_1+k_d}\Big)^2\Big(\frac{k_1}{k_2+k_d}\Big)B_0 \tag{33}$$

We can next express B_0 in terms of U_0.

$$\tfrac{d[ADP]}{dt} = k_1\Big(\tfrac{k_b}{k_d}\Big)U_0 + (k_2 - k_1)(\tfrac{k_1}{k_1+k_d})^2\tfrac{k_1}{k_2+k_d}\tfrac{k_b}{k_1+k_d}U_0$$

$$\tfrac{d[ADP]}{dt} = \tfrac{k_b}{k_d}\big(k_1 + (k_2 - k_1)\tfrac{k_d}{k_d+k_2}(\tfrac{k_1}{k_1+k_d})^3\big)U_0$$

We can then simplify this expression further using the expression $U_0 = N\big(\tfrac{k_d}{k_b+k_d}\big)$.

$$\tfrac{d[ADP]}{dt} = \tfrac{k_b}{k_d}\big(k_1 + (k_2 - k_1)\tfrac{k_d}{k_d+k_2}(\tfrac{k_1}{k_1+k_d})^3\big)N\big(\tfrac{k_d}{k_b+k_d}\big)$$

Further simplification, substitution of Eq. 1, and generalizing to n intermediate states then gives us

$$\tfrac{d[ADP]}{dt} = \Big(k_1 + (k_2 - k_1)\Big(\tfrac{k_d}{k_d+k_2}\Big)\Big(\tfrac{k_1}{k_1+k_d}\Big)^n\Big)\Big(\tfrac{[R]}{[R]+K_D}\Big)N$$

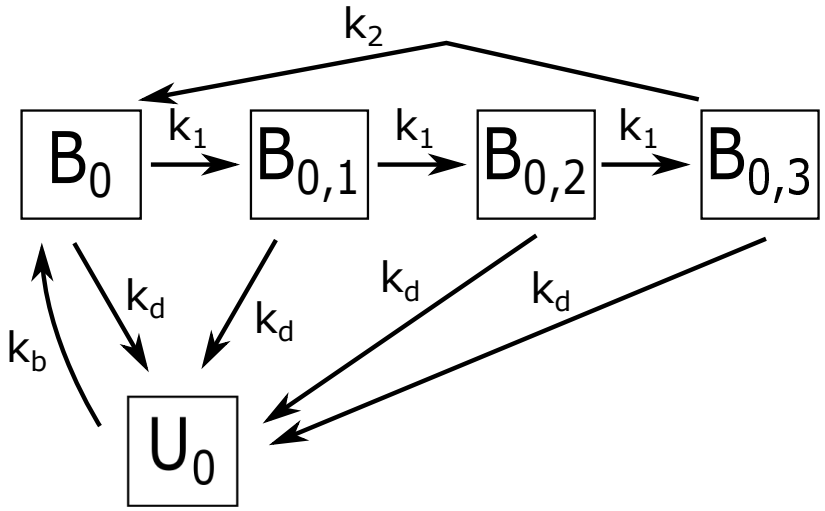

FIG. 13: A simple repositioning reaction involving 3 occurrences of a process associated with a rate constant k_1 and a single occurrence of a process associated with rate constant k_2. The variables k_d and k_b denote the microscopic dissociation and binding constants, respectively, for a remodeler interacting with the nucleosome. This model generates a steady-state ATPase production since the state $B_{0,3}$ connects to B_0.

The final term in this expression, $\left(\frac{[R]}{[R]+K_D}\right)N$, denotes the total concentration of nucleosomes bound by remodelers. Therefore, the amount of ADP per nucleosome bound remodeler increases linearly with time according to Eq. 34.

$$[ADP](t) = \left(k_1 + (k_2 - k_1)\Big(\frac{k_d}{k_d + k_2}\Big)\Big(\frac{k_1}{k_1 + k_d}\Big)^n\right)t \tag{34}$$

Alternatively, we could derive an expression for the steady-state ATPase rate using the model shown in Fig. 13. This model allows for continued nucleosome repositioning following the initial successful repositioning event and therefore does not have the strict processivity limit of the model in Fig. 12. According to the model in Fig. 13, the steady-state values of U_0, $B_{0,3}$, and B_0 are related by the following expression

$$k_B U_0 + k_2 B_{0,3} = (k_1 + k_d)B_0$$

We can rewrite this equation by expressing $B_{0,3}$ in terms of B_0.

$$k_b U_0 + k_2\big(\tfrac{k_1}{k_1+k_d}\big)^2 \tfrac{k_1}{k_2+k_d} B_0 = (k_1 + k_d)B_0$$

$$k_b U_0 = (k_1 + k_d - k_2\big(\tfrac{k_1}{k_1+k_d}\big)^2 \tfrac{k_1}{k_2+k_d})B_0$$

We can then substitute this expression into Eq. 33 and simplify using the expression $U_0 = N\big(\frac{k_d}{k_b+k_d}\big)$ to determine an equation for ATPase production. We can further generalize our result to n occurrences of the process associated with rate constant k_1. As part of this solution, we will define the parameter α using Eq. 35.

$$\alpha = \frac{1}{1 - \Big(\frac{k_2}{k_2+k_d}\Big)\Big(\frac{k_1}{k_1+k_d}\Big)^n} \tag{35}$$

The amount of ADP per nucleosome bound remodeler thus increases linearly with time according to Eq. 36.

$$[ADP](t) = \left(k_1 + (k_2 - k_1)\Big(\frac{k_d}{k_d + k_2}\Big)\Big(\frac{k_1}{k_1 + k_d}\Big)^n \alpha\right)t \tag{36}$$

Eq. 36 is identical to Eq. 11 and differs from Eq. 34 only in terms of the factor α. Furthermore, as expected from the comparison of the models in Fig. 12 and Fig, 13,

$$\lim_{k_2 \to 0} \alpha = 1$$

The parameter α can thus be interpreted as a measure of the probability that a remodeler can successfully reposition a nucleosome across multiple octamer binding sites.

It is worth noting, however, that both of these derivations ignore the possibility of a remodeler binding to a nucleosome in an orientation that does not result in subsequent repositioning; for example, the binding of U_1 to B_{1R} or U_{-1} to B_{-1L} in the model in Fig. 1. Such binding would reduce the ATPase rate since some of the remodelers would be sequestered into non-ADP-productive interactions with the nucleosomes. Furthermore, since the number of these none productive interactions remains constant but the number of productive interactions (from U_{-1} to B_{-1L} or B_{-1R} in the model in Fig. 3, *e.g.*) increase as the length of the DNA increases, we would expect the ATPase rate would similarly depend upon the length of the DNA. Therefore, since the ATPase rate associated with ISWI-catalyzed nucleosome repositioning is independent of DNA length [27], we hypothesize that the affinity of ISWI binding in non-productive interactions is less than the affinity of ISWI binding in productive interactions. Additional experiments are required to resolve this issue further.

[1] K. Luger, A. W. Mader, R. K. Richmond, D. F. Sargent, and T. J. Richmond, Nature **389**, 251 (1997).
[2] C. A. Davey, D. F. Sargent, K. Luger, A. W. Maeder, and T. J. Richmond, Journal of molecular biology **319**, 1097 (2002).
[3] T. J. Richmond and C. A. Davey, Nature **423**, 145 (2003).
[4] T. D. Frouws, S. C. Duda, and T. J. Richmond, Proceedings of the National Academy of Sciences **113**, 1214 (2016).
[5] P. Lowary and J. Widom, Journal of molecular biology **276**, 19 (1998).
[6] A. Thåström, P. Lowary, and J. Widom, Methods **33**, 33 (2004).
[7] F. Battistini, C. A. Hunter, I. K. Moore, and J. Widom, Journal of Molecular Biology **420**, 8 (2012).
[8] T. T. Ngo, J. Yoo, Q. Dai, Q. Zhang, C. He, A. Aksimentiev, and T. Ha, Nature communications **7** (2016).
[9] K. Tóth, V. Böhm, C. Sellmann, M. Danner, J. Hanne, M. Berg, I. Barz, A. Gansen, and J. Langowski, Cytometry Part A **83**, 839 (2013).
[10] J. Widom, Quarterly reviews of biophysics **34**, 269 (2001).
[11] K. Polach and J. Widom, Journal of molecular biology **254**, 130 (1995).
[12] J. Anderson and J. Widom, Journal of Molecular Biology **296**, 979 (2000).
[13] G. Li and J. Widom, Nature structural & molecular biology **11**, 763 (2004).
[14] I. F. Azmi, S. Watanabe, M. F. Maloney, S. Kang, J. A. Belsky, D. M. MacAlpine, C. L. Peterson, and S. P. Bell, eLife **6**, e22512 (2017).
[15] J. T. Kadonaga, Cell **92**, 307 (1998).
[16] C. R. Clapier and B. R. Cairns, Annual review of biochemistry **78**, 273 (2009).
[17] G. D. Bowman, Current opinion in structural biology **20**, 73 (2010).
[18] C. R. Clapier, J. Iwasa, B. R. Cairns, and C. L. Peterson, Nature Reviews Molecular Cell Biology (2017).
[19] G. Längst and P. B. Becker, Molecular cell **8**, 1085 (2001).
[20] A. Saha, J. Wittmeyer, and B. R. Cairns, Genes & development **16**, 2120 (2002).
[21] R. Strohner, M. Wachsmuth, K. Dachauer, J. Mazurkiewicz, J. Hochstatter, K. Rippe, and G. Längst, Nature structural & molecular biology **12**, 683 (2005).
[22] Y. Zhang, C. L. Smith, A. Saha, S. W. Grill, S. Mihardja, S. B. Smith, B. R. Cairns, C. L. Peterson, and C. Bustamante, Molecular cell **24**, 559 (2006).
[23] F. Mueller-Planitz, H. Klinker, J. Ludwigsen, and P. B. Becker, Nature structural & molecular biology **20**, 82 (2013).
[24] S. Deindl, W. L. Hwang, S. K. Hota, T. R. Blosser, P. Prasad, B. Bartholomew, and X. Zhuang, Cell **152**, 442 (2013).
[25] F. Mueller-Planitz, H. Klinker, and P. B. Becker, Nature structural & molecular biology **20**, 1026 (2013).
[26] K. Rippe, A. Schrader, P. Riede, R. Strohner, E. Lehmann, and G. Längst, Proceedings of the National Academy of Sciences **104**, 15635 (2007).
[27] G. Al-Ani, S. S. Malik, A. Eastlund, K. Briggs, and C. J. Fischer, Biochemistry **53**, 4346 (2014).
[28] L. Manelyte, R. Strohner, T. Gross, and G. Längst, PLoS genetics **10**, e1004157 (2014).
[29] J. Winger and G. D. Bowman, Journal of Molecular Biology **429**, 808 (2017).
[30] J. Lequieu, D. C. Schwartz, and J. J. de Pablo, Proceedings of the National Academy of Sciences , 201705685 (2017).
[31] L. Gu, M. Levitus, C. Bustamante, and J. Widom, Nature structural & molecular biology **12**, 46 (2005).
[32] Y. Lorch, B. Maier-Davis, and R. D. Kornberg, Proceedings of the National Academy of Sciences **107**, 3458 (2010).
[33] X. Liu, M. Li, X. Xia, X. Li, and Z. Chen, Nature (2017).
[34] K. K. Sinha, J. D. Gross, and G. J. Narlikar, Science **355**, eaaa3761 (2017).
[35] D. F. Corona, G. Längst, C. R. Clapier, E. J. Bonte, S. Ferrari, J. W. Tamkun, and P. B. Becker, Molecular cell **3**, 239 (1999).

[36] T. Tsukiyama, J. Palmer, C. C. Landel, J. Shiloach, and C. Wu, Genes & development **13**, 686 (1999).
[37] G. LeRoy, A. Loyola, W. S. Lane, and D. Reinberg, Journal of Biological Chemistry **275**, 14787 (2000).
[38] G. Al-Ani, K. Briggs, S. S. Malik, M. Conner, Y. Azuma, and C. J. Fischer, Biochemistry **53**, 4334 (2014).
[39] F. Reif, *Fundamentals of Statistical and Thermal Physics* (McGraw Hill, Boston, Massachusetts, 1965).
[40] S. H. Northrup and H. P. Erickson, Proceedings of the National Academy of Sciences **89**, 3338 (1992).
[41] A. Eastlund, G. Al-Ani, and C. J. Fischer, Biochimica et Biophysica Acta (BBA)-Proteins and Proteomics **1854**, 1487 (2015).
[42] G. Längst, E. J. Bonte, D. F. Corona, and P. B. Becker, Cell **97**, 843 (1999).
[43] A. L. Lucius, N. K. Maluf, C. J. Fischer, and T. M. Lohman, Biophysical journal **85**, 2224 (2003).
[44] A. Flaus, K. Luger, S. Tan, and T. J. Richmond, Proceedings of the National Academy of Sciences **93**, 1370 (1996).
[45] A. Flaus and T. J. Richmond, in *Methods in enzymology*, Vol. 304 (Elsevier, 1999) pp. 251–263.
[46] M. N. Kagalwala, B. J. Glaus, W. Dang, M. Zofall, and B. Bartholomew, The EMBO journal **23**, 2092 (2004).
[47] S. E. LeGresley, J. Wilt, and M. Antonik, Physical Review E **89**, 032708 (2014).
[48] S. Brinkers, H. R. Dietrich, F. H. de Groote, I. T. Young, and B. Rieger, The Journal of chemical physics **130**, 06B607 (2009).
[49] S. B. Smith, Y. Cui, and C. Bustamante, Science , 795 (1996).
[50] H. Chen, S. P. Meisburger, S. A. Pabit, J. L. Sutton, W. W. Webb, and L. Pollack, Proceedings of the National Academy of Sciences **109**, 799 (2012).
[51] D. R. Jacobson, D. B. McIntosh, M. J. Stevens, M. Rubinstein, and O. A. Saleh, Proceedings of the National Academy of Sciences , 201701132 (2017).
[52] S. B. Smith, L. Finzi, and C. Bustamante, Nov **13**, 1122 (1992).
[53] Y. Lu, B. Weers, and N. C. Stellwagen, Biopolymers **61**, 261 (2002).
[54] G. S. Manning, Biophysical journal **91**, 3607 (2006).
[55] J. G. Yang and G. J. Narlikar, Methods **41**, 291 (2007).
[56] P. D. Partensky and G. J. Narlikar, Journal of molecular biology **391**, 12 (2009).
[57] T. R. Blosser, J. G. Yang, M. D. Stone, G. J. Narlikar, and X. Zhuang, Nature **462**, 1022 (2009).
[58] L. R. Racki, J. G. Yang, N. Naber, P. D. Partensky, A. Acevedo, T. J. Purcell, R. Cooke, Y. Cheng, and G. J. Narlikar, Nature **462**, 1016 (2009).
[59] J. Cadet, C. Anselmino, T. Douki, and L. Voituriez, Journal of Photochemistry and Photobiology B: Biology **15**, 277 (1992).
[60] T. Mizukoshi, T. S. Kodama, Y. Fujiwara, T. Furuno, M. Nakanishi, and S. Iwai, Nucleic acids research **29**, 4948 (2001).
[61] H. Yokoyama and R. Mizutani, International journal of molecular sciences **15**, 20321 (2014).
[62] D. L. Mitchell, T. D. Nguyen, and J. E. Cleaver, Journal of Biological Chemistry **265**, 5353 (1990).
[63] J. V. Kosmoski, E. J. Ackerman, and M. J. Smerdon, Proceedings of the National Academy of Sciences **98**, 10113 (2001).
[64] C. N. Buechner, A. Maiti, A. C. Drohat, and I. Tessmer, Nucleic Acids Research **43**, 2716 (2015).
[65] C. R. Clapier, K. P. Nightingale, and P. B. Becker, Nucleic acids research **30**, 649 (2002).
[66] H. Ferreira, A. Flaus, and T. Owen-Hughes, Journal of molecular biology **374**, 563 (2007).
[67] J. A. Goldman, J. D. Garlick, and R. E. Kingston, Journal of Biological Chemistry **285**, 4645 (2010).
[68] N. Chatterjee, D. Sinha, M. Lemma-Dechassa, S. Tan, M. A. Shogren-Knaak, and B. Bartholomew, Nucleic acids research **39**, 8378 (2011).
[69] K. Polach, P. Lowary, and J. Widom, Journal of molecular biology **298**, 211 (2000).
[70] J. Anderson, P. Lowary, and J. Widom, Journal of Molecular Biology **307**, 977 (2001).
[71] L. A. Boyer, R. R. Latek, and C. L. Peterson, Nature reviews Molecular cell biology **5**, 158 (2004).
[72] M. Kasten, H. Szerlong, H. Erdjument-Bromage, P. Tempst, M. Werner, and B. R. Cairns, The EMBO journal **23**, 1348 (2004).
[73] R. J. Sims, C.-F. Chen, H. Santos-Rosa, T. Kouzarides, S. S. Patel, and D. Reinberg, Journal of Biological Chemistry **280**, 41789 (2005).
[74] J. Wysocka, T. Swigut, H. Xiao, T. A. Milne, S. Y. Kwon, J. Landry, M. Kauer, A. J. Tackett, B. T. Chait, P. Badenhorst, *et al.*, Nature **442**, 86 (2006).
[75] L. Yan, L. Wang, Y. Tian, X. Xia, and Z. Chen, Nature **540**, 466 (2016).
[76] W. Dang and B. Bartholomew, Molecular and cellular biology **27**, 8306 (2007).
[77] W. Dang, M. N. Kagalwala, and B. Bartholomew, Journal of Biological Chemistry **282**, 19418 (2007).
[78] R Core Team, *R: A Language and Environment for Statistical Computing*, R Foundation for Statistical Computing, Vienna, Austria (2013), ISBN 3-900051-07-0.